

FAST PROJECTED NEWTON-LIKE METHOD FOR PRECISION MATRIX ESTIMATION UNDER TOTAL POSITIVITY

JIAN-FENG CAI*, JOSÉ VINÍCIUS DE M. CARDOSO†, DANIEL P. PALOMAR†, AND JIAXI YING*

Abstract. We study the problem of estimating precision matrices in Gaussian distributions that are multivariate totally positive of order two (MTP₂). The precision matrix in such a distribution is an *M-matrix*. The problem can be formulated as a sign-constrained log-determinant program. The existing algorithms designed for solving this problem are based on the block coordinate descent method, which are computationally prohibitive in high-dimensional cases, because of the need to solve a large number of nonnegative quadratic programs. We propose a novel algorithm based on the two-metric projection method, with a well-designed search direction and variable partitioning scheme. Our algorithm reduces the computational complexity significantly in solving this problem, and its theoretical convergence is established. Experiments involving synthetic and real-world data demonstrate that our proposed algorithm is significantly more efficient, from a computational time perspective, than the state-of-the-art methods.

Key words. M-matrix, Two-metric projection method, Quasi-Newton method, Optimization.

AMS subject classifications. 65F30, 65Y10, 65Y20, 90C06, 90C53

1. Introduction. We consider the problem of estimating the precision matrix (*i.e.*, inverse covariance matrix) in a multivariate Gaussian distribution, where all the off-diagonal elements of the precision matrix are nonpositive. The resulting precision matrix is a symmetric *M-matrix*. Such property is also known as multivariate totally positive of order two (MTP₂) [14, 26]. For ease of presentation, we call the nonpositivity constraints on the off-diagonal elements of the precision matrix as MTP₂ constraints. This model arises in a variety of applications such as taxonomic reasoning [41], financial markets [1], factor analysis in psychometrics [26], and graph signal processing [13].

Estimating precision matrices under MTP₂ constraints has become an active research topic. Recent results provided in [26, 27, 41] show that MTP₂ constraints lead to a drastic reduction on the number of observations required for the maximum likelihood estimator (MLE) to exist in the Gaussian distribution and Ising model. Such advantages of MTP₂ constraints are critical in high-dimensional regimes, where the number of observations is usually limited compared to the problem dimension. In recent years, there is growing interest in estimating precision matrices under MTP₂ constraints in graph signal processing [13, 33, 34]. A precision matrix satisfying MTP₂ constraints can be viewed as a generalized graph Laplacian, of which the eigenvalues and eigenvectors can be interpreted as spectral frequencies and Fourier bases, thus it can be used in computing graph Fourier transform [40]. The MTP₂ property was also studied in portfolio allocation [1] and structure recovery [20, 44].

The problem of precision matrix estimation under MTP₂ constraints can be formulated as a sign-constrained log-determinant program. Recent works [13, 34, 41] proposed algorithms based on the block coordinate descent (BCD) method. Such algorithms can be efficient for low-dimensional problems, while they become time-consuming in solving high-dimensional problems, because of the need to solve a large number of nonnegative quadratic programs. Apart from BCD-type algorithms, this

*Department of Mathematics, The Hong Kong University of Science and Technology (jfcai@ust.hk, jxying@ust.hk).

†Department of Electronic and Computer Engineering, The Hong Kong University of Science and Technology (jvdmcc@connect.ust.hk, palomar@ust.hk).

sign-constrained log-determinant program may be solved by the projected gradient method, which is usually computationally efficient in each iteration. However, as a first-order method, it often suffers from the low convergence rate when solving high-dimensional optimization problems. Therefore, it remains to develop efficient and scalable algorithms for estimating the precision matrix under MTP_2 constraints.

1.1. Contributions. In this paper, we propose a fast projected Newton-like algorithm for estimating precision matrices under MTP_2 constraints. The existing algorithms [13, 34, 41] designed for solving this problem are based on the BCD method, which cyclically updates each row/column of the matrix by solving a nonnegative quadratic program. Such algorithms require $O(p^4)$ operations in each cycle, which is computationally prohibitive in high-dimensional cases. In contrast to the BCD-type algorithms [13, 34, 41], our proposed algorithm is based on the two-metric projection method. With the well-designed search direction and variable partitioning scheme, our algorithm reduces the computational complexity significantly with only $O(p^3)$ operations required in each iteration.

The theoretical convergence of the proposed algorithm is established. We prove that our algorithm converges to the minimizer of the problem of interest, and the set of *free* variables constructed by our algorithm identifies the support of the minimizer in a finite number of iterations.

Numerical experiments on both synthetic and real-world data sets provide strong evidence that our algorithm costs significantly less time to converge to the minimizer than state-of-the-art methods. Finally, we apply our method in financial time-series data, which are well-known for displaying positive dependencies, and observe a significant performance in terms of *modularity* value on the learned financial networks.

1.2. Notation and organization. Lower case bold letters denote vectors and upper case bold letters denote matrices. Both X_{ij} and $[\mathbf{X}]_{ij}$ denote the (i, j) -th entry of \mathbf{X} . $[p]$ denotes the set $\{1, \dots, p\}$, and $[p]^2$ denotes the set $\{1, \dots, p\} \times \{1, \dots, p\}$. Let \otimes be the Kronecker product and \odot be the entry-wise product. $\text{supp}(\mathbf{X}) = \{(i, j) \in [p]^2 \mid X_{ij} \neq 0\}$. $\|\mathbf{X}\|_{\max} = \max_{i,j} |X_{ij}|$ and $\|\mathbf{X}\|_{\min} = \min_{i,j} |X_{ij}|$. \mathbb{S}_+^p and \mathbb{S}_{++}^p denote the sets of symmetric positive semi-definite and positive definite matrices with dimension $p \times p$. $\text{vec}(\mathbf{X})$ and \mathbf{X}^\top denote the vectorized version and transpose of \mathbf{X} .

The paper is organized as follows. Problem formulation and related work are in section 2. Our algorithm and convergence analysis are in section 3 and section 4. Section 5 presents experimental results. Conclusions are made in section 6. The results on support recovery consistency are provided in Appendix A. The source code of our algorithm is publicly available at <https://github.com/jxying/mtp2>.

2. Problem Formulation and Related Work. In this section, we first introduce the problem formulation, then present related works.

2.1. Problem formulation. Let $\mathbf{y} = (y_1, \dots, y_p)$ be a zero-mean p -dimensional random vector following $\mathbf{y} \sim \mathcal{N}(\mathbf{0}, \Sigma)$, where Σ is the covariance matrix. We focus on the problem of estimating the precision matrix $\Theta := \Sigma^{-1}$ given n independent and identically distributed observations $\mathbf{y}^{(1)}, \dots, \mathbf{y}^{(n)}$. Let $\mathbf{S} = \frac{1}{n} \sum_{i=1}^n \mathbf{y}^{(i)} (\mathbf{y}^{(i)})^\top$ be the sample covariance matrix. Throughout the paper, the sample covariance matrix is assumed to have strictly positive diagonal elements, which holds with probability one. This is because some diagonal element S_{jj} is zero if and only if the j -th element of $\mathbf{y}^{(i)}$ must be zero for every $i \in [p]$, which holds with probability zero.

We consider solving the following sign-constrained log-determinant program:

$$(2.1) \quad \begin{aligned} \mathbf{X}^* := \arg \min_{\mathbf{X} \in \mathcal{M}^p} \quad & -\log \det(\mathbf{X}) + \text{tr}(\mathbf{X}\mathbf{S}) + \sum_{i \neq j} \lambda_{ij} |X_{ij}|, \\ \text{subject to} \quad & X_{ij} = 0, \quad \forall (i, j) \in \mathcal{E}, \end{aligned}$$

where λ_{ij} is the regularization parameter, \mathcal{E} is the disconnectivity set defined as the pairs of nodes that are forced to be disconnected, and \mathcal{M}^p is the set of all p -dimensional, symmetric, non-singular *M-matrices*, which is defined by

$$(2.2) \quad \mathcal{M}^p := \{\mathbf{X} \in \mathbb{S}_{++}^p \mid X_{ij} \leq 0, \quad \forall i \neq j\}.$$

Imposing the disconnectivity set \mathcal{E} in (2.1) ensures that the corresponding pairs of nodes are disconnected in the learned graph. The disconnectivity set can be obtained in several ways: (i) it is often the case that some edges between nodes must not exist according to prior knowledge; (ii) it can be estimated from initial estimators; (iii) it can be obtained in some tasks of learning structured graphs such as bipartite graph.

2.2. Related Work. Estimating precision matrices under Gaussian graphical models has received broad interest in optimization and machine learning. One well-known method is graphical lasso [2, 9, 36, 46], which minimizes the ℓ_1 -regularized Gaussian negative log-likelihood. Various algorithms were proposed to solve this problem including first-order methods [2, 9, 12, 15, 29, 38] and second-order methods [10, 18, 28, 43]. We note that the graphical lasso optimization problem is unconstrained and nonsmooth, while Problem (2.1) is smooth and constrained. The difficulties in solving the two problems are inherently different, and the algorithms mentioned above cannot be directly extended to solve our problem.

To estimate precision matrices under MTP_2 constraints, recent works [13, 34, 41] focused on the design of BCD-type algorithms. In [41], each column/row of the primal variable is updated at a time by solving a nonnegative quadratic program, while the remaining variable are kept fixed. All columns/rows are updated in a cycle, and the updating is repeated until convergence. The work [34] followed the similar strategy, but solved the dual problem. The resulting algorithm avoids storing a dense covariance matrix, thus can be more memory efficient. Both works [34, 41] aimed to solve Problem (2.1) without the disconnectivity constraint. More recently, a BCD-type algorithm that enables to handle the disconnectivity constraint was proposed in [13], which can be extended to estimate the precision matrix that is a diagonally dominant *M-matrix*. Regarding computational complexity, BCD-type algorithms [13, 34, 41] need to solve p nonnegative quadratic programs per cycle, and thus requires $O(p^4)$ operations in each cycle, which is computationally prohibitive in high-dimensional cases.

Our algorithm is based on the two-metric projection framework [16], which embodies two different metrics used to determine the search direction and the projection. Under this framework, a representative method is the projected Newton algorithm [6], which was originally designed for nonnegativity constrained optimization problems. However, such algorithm is not suitable to solve our problem, because it needs to store a huge Hessian matrix which requires $O(p^4)$ memory and evaluate the inverse of some principle submatrix of the Hessian which requires $O(p^6)$ operations. To reduce the computation and memory costs, the projected quasi-Newton algorithm with the limited-memory Boyden-Fletcher-Goldfarb-Shanno (L-BFGS) was proposed in [22], which uses curvature information from only the most recent iterations to construct the Hessian approximation. This algorithm only requires $O((m+p)p^2)$ operations and $O(mp^2)$ memory in each iteration, where m is the number of iterations stored

for approximating the inverse Hessian. The two-metric projection framework has been explored in many other problems such as nonnegative image reconstruction [4], nonnegative matrix approximation [21], total variation [19], image deblurring [25], phase recovery [17], and inverse heat convection [37].

3. Proposed Algorithm. In this section, we propose a fast projected Newton-like (FPN) algorithm to solve Problem (2.1).

Problem (2.1) is a constrained convex optimization problem, of which the constraints can be rewritten as $\mathbf{X} \in \Omega \cap \mathbb{S}_{++}^p$, where Ω is defined as

$$\Omega := \{\mathbf{X} \in \mathbb{R}^{p \times p} \mid X_{ij} = 0, \forall (i, j) \in \mathcal{E}; X_{ij} \leq 0, \forall i \neq j\}.$$

The set Ω is convex and closed, thus we can handle this constraint by a projection \mathcal{P}_Ω onto Ω with respect to the metric of the Frobenius norm defined by

$$(3.1) \quad [\mathcal{P}_\Omega(\mathbf{A})]_{ij} = \begin{cases} 0 & \text{if } (i, j) \in \mathcal{E}, \\ A_{ij} & \text{if } i = j, \\ \min(A_{ij}, 0) & \text{if } (i, j) \notin \mathcal{E} \text{ and } i \neq j. \end{cases}$$

But the positive definite set \mathbb{S}_{++}^p is not closed, thus cannot be handled by a projection. We impose the positive definiteness by the line search method in subsection 3.3.

To solve Problem (2.1), we start with the projected gradient method, which can be formulated as

$$(3.2) \quad \mathbf{X}_{k+1} = \mathcal{P}_\Omega(\mathbf{X}_k - \gamma_k \nabla f(\mathbf{X}_k)),$$

where γ_k is the step size, f is the objective function of Problem (2.1), and $\nabla f(\mathbf{X}_k)$ denotes the gradient at \mathbf{X}_k . The projected gradient method can be viewed as an instance of the successive convex approximation approach [39], which solves a sequence of convex approximation problems. More specifically, the iterate \mathbf{X}_{k+1} in (3.2) is the closed-form solution of the following problem:

$$(3.3) \quad \underset{\mathbf{X} \in \Omega}{\text{minimize}} \quad f(\mathbf{X}_k) + \langle \nabla f(\mathbf{X}_k), \mathbf{X} - \mathbf{X}_k \rangle + \frac{1}{2\gamma_k} \|\mathbf{X} - \mathbf{X}_k\|_{\text{F}}^2,$$

where the objective function in (3.3) is a quadratic approximation of f around the point \mathbf{X}_k . The projected gradient method is a first-order iterative method, which uses the negative gradient as the descent direction. To accelerate the convergence, one may construct a better quadratic approximation and solve the following problem:

$$(3.4) \quad \underset{\mathbf{X} \in \Omega}{\text{minimize}} \quad f(\mathbf{X}_k) + \langle \nabla f(\mathbf{X}_k), \mathbf{X} - \mathbf{X}_k \rangle + \frac{1}{2\gamma_k} \text{vec}(\mathbf{X} - \mathbf{X}_k)^\top \mathbf{M}_k \text{vec}(\mathbf{X} - \mathbf{X}_k),$$

where $\mathbf{M}_k \in \mathbb{R}^{p^2 \times p^2}$ is a positive definite symmetric matrix, and $\text{vec}(\mathbf{X}) \in \mathbb{R}^{p^2}$ denotes the vectorized version of $\mathbf{X} \in \mathbb{R}^{p \times p}$. Define a matrix $\mathbf{P}_k \in \mathbb{R}^{p \times p}$ by

$$(3.5) \quad \text{vec}(\mathbf{P}_k) = \mathbf{M}_k^{-1} \text{vec}(\nabla f(\mathbf{X}_k)).$$

Then Problem (3.4) can be equivalently expressed as

$$(3.6) \quad \underset{\mathbf{X} \in \Omega}{\text{minimize}} \quad \|\mathbf{X} - \mathbf{X}_k + \gamma_k \mathbf{P}_k\|_{\mathbf{M}_k}^2,$$

where $\|\cdot\|_{\mathbf{M}_k}$ is a quadratic norm defined by $\|\mathbf{A}\|_{\mathbf{M}_k} = \langle \text{vec}(\mathbf{A}), \mathbf{M}_k \text{vec}(\mathbf{A}) \rangle^{\frac{1}{2}}$ for any $\mathbf{A} \in \mathbb{R}^{p \times p}$. We can see that the search direction \mathbf{P}_k is induced by the metric

$\|\cdot\|_{\mathbf{M}_k}$. Such search direction enables the algorithm to achieve fast convergence by incorporating the second-order information into \mathbf{M}_k .

Unlike Problem (3.3), however, the closed-form solution for Problem (3.6) is not available because of the metric $\|\cdot\|_{\mathbf{M}_k}$. Though there are many iterative methods to solve the quadratic program (3.6), it is computationally challenging to solve (3.6) in each iteration as shown in subsection 5.1.1. To ease the computational burden, we replace $\|\cdot\|_{\mathbf{M}_k}$ in (3.6) by $\|\cdot\|_{\text{F}}$ and obtain

$$(3.7) \quad \underset{\mathbf{X} \in \Omega}{\text{minimize}} \|\mathbf{X} - \mathbf{X}_k + \gamma_k \mathbf{P}_k\|_{\text{F}}^2.$$

Then we get the closed-form solution of Problem (3.7) and establish the next iterate,

$$(3.8) \quad \mathbf{X}_{k+1} = \mathcal{P}_{\Omega}(\mathbf{X}_k - \gamma_k \mathbf{P}_k),$$

where \mathbf{P}_k denotes the search direction defined in (3.5).

Remark 3.1. We call iterate (3.8) as the two-metric projection method [16] because two different metrics are adopted, *i.e.*, the search direction \mathbf{P}_k induced by the metric of the quadratic norm $\|\cdot\|_{\mathbf{M}_k}$, and the projection \mathcal{P}_{Ω} with respect to the metric of the Frobenius norm $\|\cdot\|_{\text{F}}$. Such method has the advantage of fast convergence by incorporating second-order information when designing the direction \mathbf{P}_k , while maintaining computational efficiency of the projection \mathcal{P}_{Ω} to handle the constraints.

The iterate (3.8) needs to compute the search direction \mathbf{P}_k defined in (3.5). A straightforward implementation either relies on the inverse of \mathbf{M}_k whose dimension is $p^2 \times p^2$ or on solving a system of linear equations of the same dimension, of which the computation and memory costs are prohibitive in high-dimensional cases.

If we adopt \mathbf{M}_k as the exact Hessian matrix, then \mathbf{P}_k becomes the Newton direction and iterate (3.8) can be viewed as a natural adaptation of the unconstrained Newton's method. Interestingly, the computation and memory costs can be reduced by exploiting the structure of the Hessian of the log-determinant program [18]. More specifically, the Hessian matrix of Problem (2.1) has the following special form,

$$(3.9) \quad \mathbf{H}_k = \mathbf{X}_k^{-1} \otimes \mathbf{X}_k^{-1},$$

where \otimes denotes the Kronecker product. The following lemma shows that the computation of \mathbf{P}_k only involves the gradient calculation and matrix multiplications.

LEMMA 3.2. *If \mathbf{M}_k is constructed as the Hessian matrix \mathbf{H}_k in (3.9), then the search direction \mathbf{P}_k defined in (3.5) can be written as*

$$\mathbf{P}_k = \mathbf{X}_k \nabla f(\mathbf{X}_k) \mathbf{X}_k.$$

Proof. The Hessian matrix at \mathbf{X}_k has the form: $\mathbf{H}_k = \mathbf{X}_k^{-1} \otimes \mathbf{X}_k^{-1}$. Then we obtain $\mathbf{H}_k^{-1} = \mathbf{X}_k \otimes \mathbf{X}_k$. Following from the property of Kronecker product that $\text{vec}(\mathbf{ABC}) = (\mathbf{C}^{\top} \otimes \mathbf{A}) \text{vec}(\mathbf{B})$, we obtain

$$\text{vec}(\mathbf{P}_k) = \mathbf{H}_k^{-1} \text{vec}(\nabla f(\mathbf{X}_k)) = \text{vec}(\mathbf{X}_k \nabla f(\mathbf{X}_k) \mathbf{X}_k),$$

completing the proof. \square

Unfortunately, iterate (3.8) using the Newton direction \mathbf{P}_k from Lemma 3.2 cannot be guaranteed to converge to the minimizer because it may not be a descent iteration, which is further demonstrated by numerical results in subsection 5.1.1. Similar observations have also been reported in [6, 21].

3.1. Identifying the Sets of *Restricted* and *Free* Variables. In order to guarantee iterate (3.8) to converge to the minimizer, we partition the variables into two groups in each iteration, *i.e.*, *restricted* and *free* variables, and update the two groups separately. The *restricted* variables are directly set as zero, while the *free* variables are updated along the constructed approximate Newton direction.

We first define a set $\mathcal{T}(\mathbf{X}, \epsilon)$ with respect to $\mathbf{X} \in \mathbb{R}^{p \times p}$ and $\epsilon \in \mathbb{R}_+$,

$$(3.10) \quad \mathcal{T}(\mathbf{X}, \epsilon) := \{(i, j) \in [p]^2 \mid -\epsilon \leq X_{ij} \leq 0, [\nabla f(\mathbf{X})]_{ij} < 0\},$$

where $\nabla f(\mathbf{X})$ is the gradient in Problem (2.1). Note that for each $\mathbf{X} \in \mathcal{M}^p$, (i, j) must be the index of an off-diagonal element if $(i, j) \in \mathcal{T}(\mathbf{X}, \epsilon)$. At the $(k+1)$ -th iteration, we identify the set of *restricted* variables based on \mathbf{X}_k as follows,

$$(3.11) \quad \mathcal{I}_k := \mathcal{T}(\mathbf{X}_k, \epsilon_k) \cup \mathcal{E},$$

where \mathcal{E} is the disconnectivity set in Problem (2.1), and ϵ_k is a small positive scalar. For any $(i, j) \in \mathcal{T}(\mathbf{X}_k, \epsilon_k)$, X_{ij} in the next iterate is likely to be outside the feasible set (*i.e.*, $X_{ij} > 0$) if we remove the projection \mathcal{P}_Ω , because it is close to zero and moves towards the positive direction if using the negative of the gradient as the search direction. For any $(i, j) \in \mathcal{E}$, Problem (2.1) imposes X_{ij} to be zero. Therefore, we restrict all *restricted* variables to be zero in subsection 3.2.

To establish the theoretical convergence of the algorithm, the positive scalar ϵ_k in (3.11) is specified as

$$(3.12) \quad \epsilon_k := \min \left(2(1 - \alpha)m^2 \|\nabla f(\mathbf{X}_k)\|_{\mathcal{T}_\delta \setminus \mathcal{E}} \right),$$

where m is some positive constant as in Lemma 3.5, $\alpha \in (0, 1)$ is a parameter in the line search condition, \mathcal{T}_δ denotes the set $\mathcal{T}(\mathbf{X}_k, \delta)$, and δ is a parameter satisfying

$$(3.13) \quad 0 < \delta < \min_{(i, j) \in \text{supp}(\mathbf{X}^*)} |[\mathbf{X}^*]_{ij}|,$$

where \mathbf{X}^* is the minimizer of Problem (2.1). To ensure that Condition (3.13) holds, we can set a sufficiently small positive δ . In this case, ϵ_k in (3.12) is almost equal to δ . Then, from an implementation perspective, we can directly set a very small positive ϵ_k , and the algorithm always works well in practice.

The set of *free* variables \mathcal{I}_k^c is the complement of \mathcal{I}_k . We prove in section 4 that our variable partitioning scheme enables $\{\mathcal{I}_k^c\}$ to converge to the support of the minimizer of Problem (2.1), which in turn validates the constructions of \mathcal{I}_k and \mathcal{I}_k^c .

3.2. Computing Approximate Newton Direction. It is often the case that computing the (approximate) Newton direction needs significantly more computation than computing the gradient. However, we manage to design an approximate Newton direction that requires the same order of computation as the gradient.

We partition \mathbf{X}_k into two groups, $[\mathbf{X}_k]_{\mathcal{I}_k}$ and $[\mathbf{X}_k]_{\mathcal{I}_k^c}$, where $[\mathbf{X}_k]_{\mathcal{I}_k} \in \mathbb{R}^{|\mathcal{I}_k|}$ and $[\mathbf{X}_k]_{\mathcal{I}_k^c} \in \mathbb{R}^{|\mathcal{I}_k^c|}$ denote two vectors containing all elements of \mathbf{X}_k in the sets \mathcal{I}_k and \mathcal{I}_k^c , respectively. By permuting the entries of $\text{vec}(\mathbf{X}_k)$, we obtain the following partition,

$$(3.14) \quad \text{pvec}_k(\mathbf{X}_k) = \begin{bmatrix} [\mathbf{X}_k]_{\mathcal{I}_k^c} \\ [\mathbf{X}_k]_{\mathcal{I}_k} \end{bmatrix},$$

where $\text{pvec}_k(\mathbf{X}_k)$ stacks the elements of \mathbf{X}_k into a single vector, which is similar to $\text{vec}(\mathbf{X}_k)$, but it places the elements of \mathbf{X}_k in the sets \mathcal{I}_k^c and \mathcal{I}_k in order. Then we can rewrite the search direction \mathbf{P}_k defined in (3.5) as follows,

$$(3.15) \quad \text{pvec}_k(\mathbf{P}_k) = \mathbf{Q}_k \text{pvec}_k(\nabla f(\mathbf{X}_k)),$$

where \mathbf{Q}_k is the result of permuting the rows and columns of \mathbf{M}_k^{-1} in (3.5) corresponding to the partition in (3.14). To compute the search direction efficiently, we propose the construction of \mathbf{Q}_k and \mathbf{M}_k^{-1} as follows,

$$(3.16) \quad \mathbf{Q}_k = \begin{bmatrix} [\mathbf{M}_k^{-1}]_{\mathcal{I}_k^c \mathcal{I}_k^c} & [\mathbf{M}_k^{-1}]_{\mathcal{I}_k^c \mathcal{I}_k} \\ [\mathbf{M}_k^{-1}]_{\mathcal{I}_k \mathcal{I}_k^c} & [\mathbf{M}_k^{-1}]_{\mathcal{I}_k \mathcal{I}_k} \end{bmatrix} = \begin{bmatrix} [\mathbf{H}_k^{-1}]_{\mathcal{I}_k^c \mathcal{I}_k^c} & \mathbf{0} \\ \mathbf{0} & \mathbf{D}_k \end{bmatrix},$$

where $\mathbf{D}_k \in \mathbb{R}^{|\mathcal{I}_k| \times |\mathcal{I}_k|}$ is a positive definite diagonal matrix, and $[\mathbf{H}_k^{-1}]_{\mathcal{I}_k^c \mathcal{I}_k^c} \in \mathbb{R}^{|\mathcal{I}_k^c| \times |\mathcal{I}_k^c|}$ is a principal submatrix of \mathbf{H}_k^{-1} keeping rows and columns indexed by \mathcal{I}_k^c , in which \mathbf{H}_k is the Hessian matrix at \mathbf{X}_k . We note that the construction of \mathbf{M}_k^{-1} in (3.16) is the key step in defining the search direction, which makes the computation and memory costs comparable to the projected gradient method, while incorporating the second-order information sufficiently.

We first construct the search direction \mathbf{P}_k over the *restricted* set \mathcal{I}_k , and present the iterate $[\mathbf{X}_{k+1}]_{\mathcal{I}_k}$. Following from (3.15) and (3.16), the search direction $[\mathbf{P}_k]_{\mathcal{I}_k}$ is defined as $\mathbf{D}_k [\nabla f(\mathbf{X}_k)]_{\mathcal{I}_k}$. Since \mathbf{D}_k is a diagonal matrix, we have $[\mathbf{P}_k]_{\mathcal{I}_k} = [\tilde{\mathbf{D}}_k \odot \nabla f(\mathbf{X}_k)]_{\mathcal{I}_k}$, where \odot denotes the entry-wise product, and $\tilde{\mathbf{D}}_k$ is a $p \times p$ matrix, in which the elements $[\tilde{\mathbf{D}}_k]_{ij}$ for $(i, j) \in \mathcal{I}_k$ are from the diagonal elements of \mathbf{D}_k , and zeros for $(i, j) \in \mathcal{I}_k^c$.

For ease of presentation, by a slight abuse of notation, we write $\mathcal{P}_\Omega([\mathbf{A}]_{\mathcal{I}_k})$ for $[\mathcal{P}_\Omega(\mathbf{A})]_{\mathcal{I}_k}$. Then one has:

$$(3.17) \quad [\mathbf{X}_{k+1}]_{\mathcal{I}_k} = \mathcal{P}_\Omega\left([\mathbf{X}_k]_{\mathcal{I}_k} - \gamma_k [\tilde{\mathbf{D}}_k \odot \nabla f(\mathbf{X}_k)]_{\mathcal{I}_k}\right).$$

For each $(i, j) \in \mathcal{I}_k \setminus \mathcal{E}$, by setting

$$[\tilde{\mathbf{D}}_k]_{ij} = \frac{\epsilon_k}{\gamma_k |[\nabla f(\mathbf{X}_k)]_{ij}|},$$

we obtain $[\mathbf{X}_{k+1}]_{ij} = 0$, which follows from the definition of \mathcal{P}_Ω in (3.1). For each $(i, j) \in \mathcal{E}$, we also have $[\mathbf{X}_{k+1}]_{ij} = 0$. Note that all the indexes in \mathcal{I}_k correspond to the off-diagonal elements. To sum up, we have

$$(3.18) \quad [\mathbf{X}_{k+1}]_{\mathcal{I}_k} = \mathbf{0}.$$

We highlight that we can directly set $[\mathbf{X}_{k+1}]_{\mathcal{I}_k} = \mathbf{0}$ instead of computing $[\mathbf{X}_{k+1}]_{\mathcal{I}_k}$ according to (3.17) with an explicit $\tilde{\mathbf{D}}_k$.

Next, we compute the approximate Newton direction \mathbf{P}_k over the *free* set \mathcal{I}_k^c , and present the iterate $[\mathbf{X}_{k+1}]_{\mathcal{I}_k^c}$. We first define a projection $\mathcal{P}_{\mathcal{I}_k^c}(\mathbf{A})$ as follows,

$$(3.19) \quad [\mathcal{P}_{\mathcal{I}_k^c}(\mathbf{A})]_{ij} = \begin{cases} A_{ij} & \text{if } (i, j) \in \mathcal{I}_k^c, \\ 0 & \text{otherwise.} \end{cases}$$

Based on the well-designed gradient scaling matrix in (3.16), the proposed approximate Newton direction can be computed efficiently as shown in the following lemma.

LEMMA 3.3. *If \mathbf{M}_k is constructed by (3.16), then the search direction \mathbf{P}_k defined in (3.5) over \mathcal{I}_k^c can be written as*

$$(3.20) \quad [\mathbf{P}_k]_{\mathcal{I}_k^c} = [\mathbf{X}_k \mathcal{P}_{\mathcal{I}_k^c} (\nabla f(\mathbf{X}_k)) \mathbf{X}_k]_{\mathcal{I}_k^c}.$$

Proof. Following from (3.15) and (3.16), we obtain

$$(3.21) \quad [\mathbf{P}_k]_{\mathcal{I}_k^c} = [\mathbf{H}_k^{-1}]_{\mathcal{I}_k^c \mathcal{I}_k^c} [\nabla f(\mathbf{X}_k)]_{\mathcal{I}_k^c} = [\mathbf{H}_k^{-1} \text{vec}(\mathcal{P}_{\mathcal{I}_k^c}(\nabla f(\mathbf{X}_k)))]_{\mathcal{I}_k^c},$$

where the projection $\mathcal{P}_{\mathcal{I}_k^c}$ is defined in (3.19). Following from the fact that $\text{vec}(\mathbf{ABC}) = (\mathbf{C}^\top \otimes \mathbf{A}) \text{vec}(\mathbf{B})$ and $\mathbf{H}_k^{-1} = \mathbf{X}_k \otimes \mathbf{X}_k$, we have

$$(3.22) \quad \mathbf{H}_k^{-1} \text{vec}(\mathcal{P}_{\mathcal{I}_k^c}(\nabla f(\mathbf{X}_k))) = \text{vec}(\mathbf{X}_k \mathcal{P}_{\mathcal{I}_k^c}(\nabla f(\mathbf{X}_k)) \mathbf{X}_k).$$

We complete the proof by combining (3.21) and (3.22). \square

Using the direction $[\mathbf{P}_k]_{\mathcal{I}_k^c}$ from Lemma 3.3, we update \mathbf{X}_{k+1} over \mathcal{I}_k^c as follows,

$$(3.23) \quad [\mathbf{X}_{k+1}]_{\mathcal{I}_k^c} = \mathcal{P}_\Omega \left([\mathbf{X}_k]_{\mathcal{I}_k^c} - \gamma_k [\mathbf{X}_k \mathcal{P}_{\mathcal{I}_k^c}(\nabla f(\mathbf{X}_k)) \mathbf{X}_k]_{\mathcal{I}_k^c} \right).$$

To conclude, we update the *restricted* variables $[\mathbf{X}_{k+1}]_{\mathcal{I}_k}$ and *free* variables $[\mathbf{X}_{k+1}]_{\mathcal{I}_k^c}$ in each iteration according to (3.18) and (3.23), respectively.

3.3. Computing the Step Size. We select the step size via an Armijo-like rule that ensures the global convergence of the proposed algorithm. According to the iterate in subsection 3.2, we define $\mathbf{X}_k(\gamma_k)$ by $[\mathbf{X}_k(\gamma_k)]_{\mathcal{I}_k} = \mathbf{0}$ and

$$(3.24) \quad [\mathbf{X}_k(\gamma_k)]_{\mathcal{I}_k^c} = \mathcal{P}_\Omega \left([\mathbf{X}_k]_{\mathcal{I}_k^c} - \gamma_k [\mathbf{X}_k \mathcal{P}_{\mathcal{I}_k^c}(\nabla f(\mathbf{X}_k)) \mathbf{X}_k]_{\mathcal{I}_k^c} \right).$$

We try the step size $\gamma_k \in \{\beta^0, \beta^1, \beta^2, \dots\}$, where $\beta \in (0, 1)$ is a positive constant, until we find the smallest $t \in \mathbb{N}$ such that $\mathbf{X}_k(\gamma_k)$ with $\gamma_k = \beta^t$ satisfies that $\mathbf{X}_k(\gamma_k) \in \mathbb{S}_{++}^p$ and the line search condition below holds:

$$(3.25) \quad f(\mathbf{X}_k(\gamma_k)) \leq f(\mathbf{X}_k) - \alpha \gamma_k \langle [\nabla f(\mathbf{X}_k)]_{\mathcal{I}_k^c}, [\mathbf{P}_k]_{\mathcal{I}_k^c} \rangle - \alpha \langle [\nabla f(\mathbf{X}_k)]_{\mathcal{I}_k}, [\mathbf{X}_k]_{\mathcal{I}_k} \rangle,$$

where $\alpha \in (0, 1)$ is a scalar. Then we set $\mathbf{X}_{k+1} = \mathbf{X}_k(\gamma_k)$. The positive definiteness of \mathbf{X}_{k+1} can be verified when computing the Cholesky factorization for evaluating the objective function. The proposed algorithm is summarized in Algorithm 3.1.

The line search condition (3.25) is a variant of the Armijo rule. In what follows, we show that the condition (3.25) is always satisfied for a small enough step size in Proposition 3.4 and the objective function is guaranteed to decrease in Proposition 3.6.

We first define the feasible set of Problem (2.1) as

$$(3.26) \quad \mathcal{U}^p := \{ \mathbf{X} \in \mathbb{R}^{p \times p} \mid \mathbf{X} \in \mathcal{M}^p, X_{ij} = 0, \forall (i, j) \in \mathcal{E} \}.$$

It is obvious that the set \mathcal{U}^p is convex. Consider a point $\mathbf{X}^o \in \mathcal{U}^p$, and define the lower level set of the objective f of Problem (2.1) as

$$(3.27) \quad L_f := \{ \mathbf{X} \in \mathcal{U}^p \mid f(\mathbf{X}) \leq f(\mathbf{X}^o) \}.$$

PROPOSITION 3.4. *For any $\mathbf{X}_k \in L_f$, there exists a $\bar{\gamma}_k > 0$ such that $\mathbf{X}_k(\gamma_k) \in \mathbb{S}_{++}^p$ and the line search condition (3.25) holds for any $\gamma_k \in (0, \bar{\gamma}_k)$.*

Algorithm 3.1 Fast Projected Newton-like (FPN) algorithm

1: **Input:** Regularization parameter λ_{ij} , \mathbf{S} , \mathbf{X}_0 , α , and β ;
2: **for** $k = 0, 1, 2, \dots$ **do**
3: Identify the *restricted* set \mathcal{I}_k and *free* set \mathcal{I}_k^c according to (3.11);
4: Compute the approximate Newton direction over the set \mathcal{I}_k^c :

$$[\mathbf{P}_k]_{\mathcal{I}_k^c} = [\mathbf{X}_k \mathcal{P}_{\mathcal{I}_k^c}(\nabla f(\mathbf{X}_k)) \mathbf{X}_k]_{\mathcal{I}_k^c};$$

5: $t \leftarrow 0$;
6: **repeat**
7: Update \mathbf{X}_{k+1} : $[\mathbf{X}_{k+1}]_{\mathcal{I}_k} = \mathbf{0}$, and $[\mathbf{X}_{k+1}]_{\mathcal{I}_k^c} = \mathcal{P}_{\Omega}([\mathbf{X}_k]_{\mathcal{I}_k^c} - \beta^t [\mathbf{P}_k]_{\mathcal{I}_k^c})$;
8: $t \leftarrow t + 1$;
9: **until** $\mathbf{X}_{k+1} \succ \mathbf{0}$, and

$$f(\mathbf{X}_{k+1}) \leq f(\mathbf{X}_k) - \alpha \beta^t \langle [\nabla f(\mathbf{X}_k)]_{\mathcal{I}_k^c}, [\mathbf{P}_k]_{\mathcal{I}_k^c} \rangle - \alpha \langle [\nabla f(\mathbf{X}_k)]_{\mathcal{I}_k}, [\mathbf{X}_k]_{\mathcal{I}_k} \rangle.$$

10: **end for**

To prove Proposition 3.4, we first establish Lemma 3.5 below to show that the lower level set of the objective function is compact. We note that Lemma 3.5 depends on the condition that the sample covariance matrix has strictly positive diagonal elements, which is assumed throughout the paper and holds with probability one.

LEMMA 3.5. *The lower level set L_f defined in (3.27) is nonempty and compact, and for any $\mathbf{X} \in L_f$, we have*

$$m\mathbf{I} \preceq \mathbf{X} \preceq M\mathbf{I},$$

for some positive constants m and M .

Proof. We first show that the largest eigenvalue of any $\mathbf{X} \in L_f$ can be upper bounded by M . The objective function of (2.1) can be written as

$$f(\mathbf{X}) = -\log \det(\mathbf{X}) + \text{tr}(\mathbf{X}\mathbf{G}),$$

where $\mathbf{G} = \mathbf{S} - \boldsymbol{\lambda}$ with $\boldsymbol{\lambda}$ defined by

$$(3.28) \quad [\boldsymbol{\lambda}]_{ij} = \begin{cases} \lambda_{ij} & \text{if } i \neq j, \\ 0 & \text{otherwise.} \end{cases}$$

Define two constants

$$\mu := \min_i G_{ii}, \quad \text{and} \quad v := \max_{i \neq j, (i,j) \notin \mathcal{E}} |G_{ij}|.$$

Note that $\mu > 0$ because $S_{ii} > 0$ for each $i \in [p]$. Then one has

$$(3.29) \quad \text{tr}(\mathbf{X}\mathbf{G}) = \sum_i G_{ii}X_{ii} + \sum_{i \neq j} G_{ij}X_{ij} \geq \mu \text{tr}(\mathbf{X}) + v \sum_{i \neq j} X_{ij},$$

where the inequality follows from the fact that $X_{ij} \leq 0$ for $i \neq j$, and $X_{ij} = 0$ for $(i,j) \in \mathcal{E}$. We denote the largest eigenvalue of \mathbf{X} by $\lambda_{\max}(\mathbf{X})$. Then we have

$$(3.30) \quad \lambda_{\max}(\mathbf{X}) \leq \text{tr}(\mathbf{X}) \leq \frac{1}{\mu} \left(\text{tr}(\mathbf{X}\mathbf{G}) + v \sum_{i \neq j} |X_{ij}| \right),$$

where the second inequality follows from (3.29). In what follows, we bound the terms $\text{tr}(\mathbf{X}\mathbf{G})$ and $\sum_{i \neq j} X_{ij}$. For any $\mathbf{X} \in L_f$, one has $f(\mathbf{X}^o) \geq -\log \det(\mathbf{X}) + \text{tr}(\mathbf{X}\mathbf{G})$. Therefore, the term $\text{tr}(\mathbf{X}\mathbf{G})$ can be bounded by

$$(3.31) \quad \text{tr}(\mathbf{X}\mathbf{G}) \leq f(\mathbf{X}^o) + \log \det(\mathbf{X}) \leq f(\mathbf{X}^o) + p \log(\lambda_{\max}(\mathbf{X})).$$

Let $\lambda' := \min_{i \neq j, (i,j) \notin \mathcal{E}} \lambda_{ij}$. Then one has

$$(3.32) \quad \sum_{i \neq j} |X_{ij}| \leq \frac{1}{\lambda'} \sum_{i \neq j} \lambda_{ij} |X_{ij}| \leq \frac{1}{\lambda'} (f(\mathbf{X}^o) + p \log(\lambda_{\max}(\mathbf{X}))),$$

where the last inequality follows from $\sum_{i \neq j} \lambda_{ij} |X_{ij}| \leq \text{tr}(\mathbf{X}\mathbf{G})$, because $\text{tr}(\mathbf{X}\mathbf{S}) \geq 0$ since $\mathbf{X} \in \mathbb{S}_{++}^p$ and $\mathbf{S} \in \mathbb{S}_+^p$. Together with (3.30), (3.31) and (3.32), we obtain

$$\lambda_{\max}(\mathbf{X}) \leq \frac{1}{\mu} \left(1 + \frac{v}{\lambda'} \right) (f(\mathbf{X}^o) + p \log(\lambda_{\max}(\mathbf{X}))).$$

Since $\log(\lambda_{\max}(\mathbf{X}))$ grows much slower than $\lambda_{\max}(\mathbf{X})$, $\lambda_{\max}(\mathbf{X})$ can be upper bounded by a constant M , which depends on $f(\mathbf{X}^o)$, \mathbf{S} , and $\boldsymbol{\lambda}$.

We denote the smallest eigenvalue of \mathbf{X} by $\lambda_{\min}(\mathbf{X})$. For any $\mathbf{X} \in L_f$, one has

$$f(\mathbf{X}^o) \geq f(\mathbf{X}) \geq -\log \det(\mathbf{X}) \geq -\log \lambda_{\min}(\mathbf{X}) - (p-1) \log M.$$

As a result, we have $\lambda_{\min}(\mathbf{X}) \geq e^{-f(\mathbf{X}^o)} M^{-(p-1)}$, which shows that $\lambda_{\min}(\mathbf{X})$ can be lower bounded by a positive constant $m = e^{-f(\mathbf{X}^o)} M^{-(p-1)}$. Finally, we show that the lower level set L_f is compact. First, L_f is closed because f is a continuous function. Second, L_f is also bounded because it is a subset of $\{\mathbf{X} \in \mathbb{R}^{p \times p} \mid m\mathbf{I} \preceq \mathbf{X} \preceq M\mathbf{I}\}$. \square

Proof of Proposition 3.4. We first show that $\mathbf{X}_k(\gamma_k) \in \mathbb{S}_{++}$ holds for a small enough step size. The $\mathbf{X}_k(\gamma_k)$ can be equivalently written in the form $\mathbf{X}_k(\gamma_k) = \mathbf{Z}_k - \gamma_k \mathbf{G}_k$, where $\mathbf{Z}_k \in \mathbb{R}^{p \times p}$ defined by $[\mathbf{Z}_k]_{ij} = [\mathbf{X}_k]_{ij}$ if $(i, j) \in \mathcal{I}_k^c$, and 0 otherwise. \mathbf{G}_k is some search direction only over \mathcal{I}_k^c , which is a symmetric matrix. It is known that a matrix \mathbf{A} is a nonsingular *M-matrix* if and only if \mathbf{A} is a *Z-matrix* and there exists a vector $\mathbf{x} > \mathbf{0}$ with $\mathbf{A}\mathbf{x} > \mathbf{0}$ [35]. Following from the fact that \mathbf{X}_k is a nonsingular *M-matrix*, there exists $\mathbf{x} > \mathbf{0}$ such that

$$\mathbf{Z}_k \mathbf{x} \geq \mathbf{X}_k \mathbf{x} > 0.$$

Therefore, \mathbf{Z}_k is also a nonsingular *M-matrix*, implying that $\mathbf{Z}_k \in \mathbb{S}_{++}$. As a result, if $\gamma_k < \lambda_{\min}(\mathbf{Z}_k)/\rho(\mathbf{G}_k)$, where $\rho(\mathbf{G}_k)$ is the spectral radius of \mathbf{G}_k , then $\mathbf{X}_k(\gamma_k) \in \mathbb{S}_{++}$. The definition of $\mathbf{X}_k(\gamma_k)$ further guarantees that $\mathbf{X}_k(\gamma_k) \in \mathcal{U}^p$. We can verify that $f(\mathbf{X}) = +\infty$ for any $\mathbf{X} \in \text{cl}(\mathcal{U}^p) \setminus \mathcal{U}^p$, where \mathbf{X} is positive semidefinite and singular. Thus, we consider an $\mathbf{X}^o \in \mathcal{U}^p$ with $f(\mathbf{X}^o)$ sufficiently large such that $f(\mathbf{X}_k(\gamma_k)) \leq f(\mathbf{X}^o)$. Therefore, $\mathbf{X}_k(\gamma_k) \in L_f$.

Next we prove that the line search condition (3.25) holds for a small enough step size. Recall that \mathcal{I}_k^c is the complement of the set \mathcal{I}_k defined in (3.11). For any $\mathbf{X}_k \in L_f$, the set \mathcal{I}_k^c can be represented as

$$\mathcal{I}_k^c = \mathcal{T}^c(\mathbf{X}_k, \epsilon_k) \cap \mathcal{E}^c = \bigcup_{l=1}^5 \mathcal{B}_k^{(l)},$$

where $\mathcal{B}_k^{(l)}$, $l = 1, \dots, 5$, are defined as

$$\begin{aligned}\mathcal{B}_k^{(1)} &= \{(i, j) \in \mathcal{E}^c \mid -\epsilon_k \leq [\mathbf{X}_k]_{ij} \leq 0, [\nabla f(\mathbf{X}_k)]_{ij} \geq 0, [\mathbf{P}_k]_{ij} < 0\}, \\ \mathcal{B}_k^{(2)} &= \{(i, j) \in \mathcal{E}^c \mid -\epsilon_k \leq [\mathbf{X}_k]_{ij} \leq 0, [\nabla f(\mathbf{X}_k)]_{ij} \geq 0, [\mathbf{P}_k]_{ij} \geq 0\}, \\ \mathcal{B}_k^{(3)} &= \{(i, j) \in \mathcal{E}^c \mid [\mathbf{X}_k]_{ij} < -\epsilon_k, [\mathbf{P}_k]_{ij} < 0\}, \\ \mathcal{B}_k^{(4)} &= \{(i, j) \in \mathcal{E}^c \mid [\mathbf{X}_k]_{ij} < -\epsilon_k, [\mathbf{P}_k]_{ij} \geq 0\}, \\ \mathcal{B}_k^{(5)} &= \{(i, j) \in \mathcal{E}^c \mid [\mathbf{X}_k]_{ij} > 0\}.\end{aligned}$$

Each subset $\mathcal{B}_k^{(l)}$ is disjoint with each other. $\mathcal{B}_k^{(5)}$ only contains the indexes of the diagonal elements of \mathbf{X}_k , while the other subsets include the indexes of the off-diagonal elements. Then one has, for any $(i, j) \in \mathcal{B}_k^{(1)}$ and $\gamma_k > 0$,

$$(3.33) \quad 0 \leq [\mathbf{X}_k(\gamma_k)]_{ij} - [\mathbf{X}_k]_{ij} = [\mathcal{P}_\Omega(\mathbf{X}_k - \gamma_k \mathbf{P}_k)]_{ij} - [\mathbf{X}_k]_{ij} \leq -\gamma_k [\mathbf{P}_k]_{ij}.$$

For any $(i, j) \in \mathcal{B}_k^{(2)}$ and $\gamma_k > 0$, one has $[\mathbf{X}_k(\gamma_k)]_{ij} - [\mathbf{X}_k]_{ij} = -\gamma_k [\mathbf{P}_k]_{ij}$. For any $(i, j) \in \mathcal{B}_k^{(3)}$, if the step size satisfies

$$(3.34) \quad 0 < \gamma_k \leq \min_{(i, j) \in \mathcal{B}_k^{(3)}} \frac{\epsilon_k}{|[\mathbf{P}_k]_{ij}|},$$

then one has $[\mathbf{X}_k(\gamma_k)]_{ij} - [\mathbf{X}_k]_{ij} = -\gamma_k [\mathbf{P}_k]_{ij}$. Similarly, for any $(i, j) \in \mathcal{B}_k^{(4)}$ and $\gamma_k > 0$, $[\mathbf{X}_k(\gamma_k)]_{ij} - [\mathbf{X}_k]_{ij} = -\gamma_k [\mathbf{P}_k]_{ij}$. Finally, for any $(i, j) \in \mathcal{B}_k^{(5)}$, $[\mathbf{X}_k]_{ij}$ must be on the diagonal of \mathbf{X}_k . Therefore, we can directly remove the projection \mathcal{P}_Ω , and obtain $[\mathbf{X}_k(\gamma_k)]_{ij} - [\mathbf{X}_k]_{ij} = -\gamma_k [\mathbf{P}_k]_{ij}$. Therefore, if (3.34) holds, one has

$$(3.35) \quad \langle [\nabla f(\mathbf{X}_k)]_{\mathcal{I}_k^c}, [\mathbf{X}_k(\gamma_k)]_{\mathcal{I}_k^c} - [\mathbf{X}_k]_{\mathcal{I}_k^c} \rangle \leq -\gamma_k \langle [\nabla f(\mathbf{X}_k)]_{\mathcal{I}_k^c}, [\mathbf{P}_k]_{\mathcal{I}_k^c} \rangle,$$

where the inequality follows from (3.33). One also has

$$(3.36) \quad \|\mathbf{X}_k(\gamma_k) - \mathbf{X}_k\|_F^2 \leq \gamma_k^2 \langle [\mathbf{P}_k]_{\mathcal{I}_k^c}, [\mathbf{P}_k]_{\mathcal{I}_k^c} \rangle + a_k \langle [\nabla f(\mathbf{X}_k)]_{\mathcal{I}_k}, [\mathbf{X}_k]_{\mathcal{I}_k} \rangle,$$

where $a_k = \frac{\epsilon_k}{\|[\nabla f(\mathbf{X}_k)]_{\mathcal{I}_k \setminus \mathcal{E}}\|_{\min}}$, and the inequality follows from the fact that $[\mathbf{X}_k(\gamma_k)]_{\mathcal{I}_k} = \mathbf{0}$. Note that $\mathcal{I}_k = \mathcal{T}_k \cup \mathcal{E}$, and $[\mathbf{X}_k]_{ij} = [\mathbf{X}_k(\gamma_k)]_{ij} = 0$ for any $(i, j) \in \mathcal{E}$. Moreover, one has

$$(3.37) \quad \begin{aligned}\langle [\mathbf{P}_k]_{\mathcal{I}_k^c}, [\mathbf{P}_k]_{\mathcal{I}_k^c} \rangle &\leq \|[\mathbf{M}_k^{-1}]_{\mathcal{I}_k^c \mathcal{I}_k^c}^{\frac{1}{2}}\|_2^2 \|[\mathbf{M}_k^{-1}]_{\mathcal{I}_k^c \mathcal{I}_k^c}^{\frac{1}{2}} [\nabla f(\mathbf{X}_k)]_{\mathcal{I}_k^c}\|^2 \\ &= \lambda_{\max}([\mathbf{M}_k^{-1}]_{\mathcal{I}_k^c \mathcal{I}_k^c}) \langle [\nabla f(\mathbf{X}_k)]_{\mathcal{I}_k^c}, [\mathbf{P}_k]_{\mathcal{I}_k^c} \rangle.\end{aligned}$$

The largest eigenvalue of $[\mathbf{M}_k^{-1}]_{\mathcal{I}_k^c \mathcal{I}_k^c}$ can be bounded by

$$(3.38) \quad \lambda_{\max}([\mathbf{M}_k^{-1}]_{\mathcal{I}_k^c \mathcal{I}_k^c}) \leq \lambda_{\max}(\mathbf{H}_k^{-1}) = \lambda_{\max}(\mathbf{X}_k \otimes \mathbf{X}_k) \leq M^2,$$

where the first inequality follows from the Eigenvalue Interlacing Theorem, and the second inequality follows from Lemma 3.5. Combining (3.36), (3.37) and (3.38) yields

$$\|\mathbf{X}_k(\gamma_k) - \mathbf{X}_k\|_F^2 \leq \gamma_k^2 M^2 \langle [\nabla f(\mathbf{X}_k)]_{\mathcal{I}_k^c}, [\mathbf{P}_k]_{\mathcal{I}_k^c} \rangle + a_k \langle [\nabla f(\mathbf{X}_k)]_{\mathcal{I}_k}, [\mathbf{X}_k]_{\mathcal{I}_k} \rangle.$$

Since $\mathbf{X}_k(\gamma_k) \in L_f$, we obtain

$$(3.39) \quad f(\mathbf{X}_k(\gamma_k)) - f(\mathbf{X}_k) \leq \langle \nabla f(\mathbf{X}_k), \mathbf{X}_k(\gamma_k) - \mathbf{X}_k \rangle + \frac{1}{2m^2} \|\mathbf{X}_k(\gamma_k) - \mathbf{X}_k\|_F^2,$$

where the inequality follows from

$$\lambda_{\max}(\nabla^2 f(\mathbf{X})) = \lambda_{\max}(\mathbf{X}^{-1} \otimes \mathbf{X}^{-1}) = \lambda_{\max}^2(\mathbf{X}^{-1}) \leq \frac{1}{m^2}, \quad \forall \mathbf{X} \in L_f,$$

where the inequality follows from Lemma 3.5.

Let $\bar{\gamma}_k = \min\left(\frac{2(1-\alpha)m^2}{M^2}, \min_{(i,j) \in \mathcal{B}_k^{(3)}} \frac{\epsilon_k}{|[\mathbf{P}_k]_{ij}|}, \frac{\lambda_{\min}(\mathbf{Z}_k)}{\rho(\mathbf{G}_k)}\right)$. Note that $\bar{\gamma}_k$ is bounded away from zero, because each $[\mathbf{P}_k]_{ij}$ is bounded following from Lemma 3.5. To this end, for any $\gamma_k \in (0, \bar{\gamma}_k)$,

$$(3.40) \quad f(\mathbf{X}_k(\gamma_k)) - f(\mathbf{X}_k) \leq -\alpha\gamma_k \langle [\nabla f(\mathbf{X}_k)]_{\mathcal{I}_k^c}, [\mathbf{P}_k]_{\mathcal{I}_k^c} \rangle - \alpha \langle [\nabla f(\mathbf{X}_k)]_{\mathcal{I}_k}, [\mathbf{X}_k]_{\mathcal{I}_k} \rangle,$$

where the inequality follows from (3.35), the definition of ϵ_k in (3.12), the inequality $\|[\nabla f(\mathbf{X}_k)]_{\mathcal{T}_\delta \setminus \mathcal{E}}\|_{\min} \leq \|[\nabla f(\mathbf{X}_k)]_{\mathcal{T}_k \setminus \mathcal{E}}\|_{\min}$, because $\mathcal{T}_k \subseteq \mathcal{T}_\delta$, and the inequality $\langle [\nabla f(\mathbf{X}_k)]_{\mathcal{I}_k^c}, [\mathbf{P}_k]_{\mathcal{I}_k^c} \rangle \geq 0$, because $[\mathbf{M}_k^{-1}]_{\mathcal{I}_k^c \mathcal{I}_k^c}$ is positive definite and

$$(3.41) \quad \langle [\nabla f(\mathbf{X}_k)]_{\mathcal{I}_k^c}, [\mathbf{P}_k]_{\mathcal{I}_k^c} \rangle = \langle [\nabla f(\mathbf{X}_k)]_{\mathcal{I}_k^c}, [\mathbf{M}_k^{-1}]_{\mathcal{I}_k^c \mathcal{I}_k^c} [\nabla f(\mathbf{X}_k)]_{\mathcal{I}_k^c} \rangle. \quad \square$$

The following proposition shows that $\mathbf{X}_k(\gamma_k)$ leads to a sufficient decrease of the objective function value.

PROPOSITION 3.6. *For any $\mathbf{X}_k \in L_f$, if $\mathbf{X}_k(\gamma_k)$ satisfies the line search condition (3.25), then we have*

$$f(\mathbf{X}_k(\gamma_k)) \leq f(\mathbf{X}_k) - \alpha\gamma_k m^2 \|\nabla f(\mathbf{X}_k)\|_{\mathcal{I}_k^c}^2,$$

where m is defined in Lemma 3.5.

Proof. The line search condition (3.25) leads to

$$(3.42) \quad f(\mathbf{X}_k(\gamma_k)) - f(\mathbf{X}_k) \leq -\alpha\gamma_k \langle [\nabla f(\mathbf{X}_k)]_{\mathcal{I}_k^c}, [\mathbf{M}_k^{-1}]_{\mathcal{I}_k^c \mathcal{I}_k^c} [\nabla f(\mathbf{X}_k)]_{\mathcal{I}_k^c} \rangle,$$

where the inequality follows from $\langle [\nabla f(\mathbf{X}_k)]_{\mathcal{I}_k}, [\mathbf{X}_k]_{\mathcal{I}_k} \rangle \geq 0$. We further have

$$(3.43) \quad \lambda_{\min}([\mathbf{M}_k^{-1}]_{\mathcal{I}_k^c \mathcal{I}_k^c}) \geq \lambda_{\min}(\mathbf{H}_k^{-1}) = \lambda_{\min}(\mathbf{X}_k \otimes \mathbf{X}_k) \geq m^2,$$

where the first and second inequalities follow from Eigenvalue Interlacing Theorem and Lemma 3.5, respectively. We complete the proof by combining (3.42) and (3.43). \square

3.4. Computational Complexity. It is observed in Lemma 3.3 that, to compute the approximate Newton direction, our algorithm needs to compute the gradient $\nabla f(\mathbf{X}_k)$, two matrix multiplications, and one projection, whose computational costs are $O(p^3)$, $O(p^3)$, and $O(p^2)$, respectively. Therefore, the computational complexity of our algorithm is $O(p^3)$ in computing the search direction, which is the same as that of the projected gradient method. Since our algorithm exploits the benefits of the second-order information when defining the search direction, it shows a faster convergence than the projected gradient method.

The Cholesky factorization, which requires $O(p^3)$ operations, is needed in evaluating the objective function of Problem (2.1), and that dominates the computational cost in the line search method. Note that the line search is typically needed for other gradient or Newton-based algorithms to adaptively choose the step size.

In summary, the overall computational complexity of our algorithm is $O(p^3)$ per iteration. Recall that BCD-type algorithms [13, 34, 41] require $O(p^4)$ operations in each cycle, and the projected quasi-Newton with L-BFGS [22] requires $O((m + p)p^2)$ operations per iteration, where m is the number of iterations stored for approximating the inverse Hessian. In addition, our algorithm requires $O(p^2)$ memory that is the same as those of the projected gradient method and BCD-type algorithms [13, 34, 41], while the projected quasi-Newton with L-BFGS [22] requires $O(mp^2)$ memory.

Remark 3.7. The design of our algorithm is inspired by the projected Newton method [6], which is originally proposed for solving general nonnegativity constrained problems. The significant differences between our algorithm and the method in [6] are in the design of the search direction and variable partitioning scheme. Our well-designed search direction and partitioning scheme lead to our algorithm to be very efficient, while the projected Newton method in [6] requires $O(p^6)$ operations and $O(p^4)$ memory in each iteration for solving Problem (2.1). Such complexities cannot be reduced through exploiting the special structure of the Hessian. In addition, our partitioning scheme is able to handle the zero pattern equality constraint, while that is not the case for the method in [6].

4. Convergence Analysis. We first show that the minimizer of Problem (2.1) is unique. We note that the following theorem relies on the condition that the diagonal elements of the sample covariance matrix \mathbf{S} are strictly positive, which is assumed throughout the paper and holds with probability one.

THEOREM 4.1. *The minimizer of Problem (2.1) is unique, and a point $\mathbf{X}^* \in \mathcal{M}^p$ is the minimizer if and only if it satisfies*

$$(4.1) \quad [\mathbf{X}^*]_{ij} = 0 \quad \forall (i, j) \in \mathcal{E}, \quad [\nabla f(\mathbf{X}^*)]_{\mathcal{V} \setminus \mathcal{E}} \leq \mathbf{0}, \quad \text{and} \quad [\nabla f(\mathbf{X}^*)]_{\mathcal{V}^c} = \mathbf{0},$$

where $\mathcal{V} = \{(i, j) \in [p]^2 \mid [\mathbf{X}^*]_{ij} = 0\}$.

Proof. We first prove that Problem (2.1) has at least one minimizer. It is known by the Weierstrass' extreme value theorem [11] that the set of minima is nonempty for any lower semicontinuous function with a nonempty compact lower level set. Therefore, the existence of the minimizers for Problem (2.1) can be guaranteed by Lemma 3.5.

On the other hand, we show that Problem (2.1) has at most one minimizer by its strict convexity. We have $\nabla^2 f(\mathbf{X}) = \mathbf{X}^{-1} \otimes \mathbf{X}^{-1}$. Thus $\nabla^2 f(\mathbf{X}) \succ \mathbf{0}$ for any \mathbf{X} in the feasible region of Problem (2.1) defined in (3.26). Therefore, Problem (2.1) is strictly convex, and thus has at most one minimizer. Together with the existence of the minimizers, we conclude that Problem (2.1) has an unique minimizer.

The Lagrangian of Problem (2.1) is

$$(4.2) \quad \mathcal{L}(\mathbf{X}, \mathbf{Y}) = -\log \det(\mathbf{X}) + \text{tr}(\mathbf{X}\mathbf{S}) + \langle \mathbf{Y} - \boldsymbol{\lambda}, \mathbf{X} \rangle,$$

where \mathbf{Y} is a KKT multiplier with $Y_{ii} = 0$ for $i \in [p]$, and $\boldsymbol{\lambda}$ is defined in (3.28).

For a convex optimization problem with Slater's condition holding, a pair is primal and dual optimal if and only if the KKT conditions hold. Thus, $(\mathbf{X}^*, \mathbf{Y}^*)$ is primal

and dual optimal if and only if it satisfies the KKT conditions of (2.1) as below,

$$(4.3) \quad -(\mathbf{X}^*)^{-1} + \mathbf{S} - \boldsymbol{\lambda} + \mathbf{Y}^* = \mathbf{0};$$

$$(4.4) \quad X_{ij}^* = 0, \quad \forall (i, j) \in \mathcal{E};$$

$$(4.5) \quad X_{ij}^* Y_{ij}^* = 0, \quad X_{ij}^* \leq 0, \quad Y_{ij}^* \geq 0, \quad \forall i \neq j \text{ and } (i, j) \notin \mathcal{E};$$

$$(4.6) \quad Y_{ii}^* = 0, \quad \forall i \in [p].$$

We first prove that the minimizer \mathbf{X}^* must satisfy all conditions in (4.1). Note that the KKT conditions (4.3)-(4.6) must hold for the minimizer \mathbf{X}^* . Let $\mathcal{V} = \{(i, j) \in [p]^2 \mid X_{ij}^* = 0\}$. First, $X_{ij}^* = 0$ for any $(i, j) \in \mathcal{E}$ following from (4.4). Second, for any (i, j) with $i \neq j$ and $(i, j) \in \mathcal{V}^c$, we have $X_{ij}^* \neq 0$ and $(i, j) \notin \mathcal{E}$. Following from (4.5), we further obtain $Y_{ij}^* = 0$. Together with (4.6), we conclude that $Y_{ij}^* = 0$ for any $(i, j) \in \mathcal{V}^c$. Following from (4.3), $[\nabla f(\mathbf{X}^*)]_{\mathcal{V}^c} = \mathbf{0}$. Since \mathbf{X}^* is positive definite, $(i, i) \in \mathcal{V}^c$ for any $i \in [p]$. Then, for any $(i, j) \in \mathcal{V} \setminus \mathcal{E}$, we have $i \neq j$, thus obtain $Y_{ij}^* \geq 0$ according to (4.5). Following from (4.3), we get $[\nabla f(\mathbf{X}^*)]_{\mathcal{V} \setminus \mathcal{E}} \leq \mathbf{0}$.

Now we prove that any point $\mathbf{X}^* \in \mathcal{M}^p$ satisfying the conditions in (4.1) must be the minimizer, *i.e.*, the KKT conditions (4.3)-(4.6) hold for \mathbf{X}^* . We construct \mathbf{Y}^* by $\mathbf{Y}^* = -\nabla f(\mathbf{X}^*)$. First, it is straightforward to check that the conditions (4.3) and (4.4) hold. Second, we have

$$(4.7) \quad [\mathbf{Y}^*]_{\mathcal{V}^c} = -[\nabla f(\mathbf{X}^*)]_{\mathcal{V}^c} = \mathbf{0}.$$

We know that $(i, i) \in \mathcal{V}^c$ for any $i \in [p]$, since $\mathbf{X}^* \in \mathcal{M}^p$. Together with (4.7), we obtain that the condition (4.6) holds.

Finally, following from the fact that $(i, i) \in \mathcal{V}^c$ for any $i \in [p]$ and $\mathcal{E} \subseteq \mathcal{V}$, we obtain $\{(i, j) \in [p]^2 \mid i \neq j, (i, j) \notin \mathcal{E}\} = \mathcal{I}_1 \cup \mathcal{I}_2$, where $\mathcal{I}_1 = \{(i, j) \in [p]^2 \mid (i, j) \in \mathcal{V}^c, i \neq j\}$, and $\mathcal{I}_2 = \{(i, j) \in [p]^2 \mid (i, j) \in \mathcal{V}, (i, j) \notin \mathcal{E}\}$. For any $(i, j) \in \mathcal{I}_1$, we have $Y_{ij}^* = 0$ according to (4.7), and $X_{ij}^* < 0$ since $\mathbf{X}^* \in \mathcal{M}^p$. Thus the condition (4.5) holds for any $(i, j) \in \mathcal{I}_1$. For any $(i, j) \in \mathcal{I}_2$, we have $X_{ij}^* = 0$, and $Y_{ij}^* = -[\nabla f(\mathbf{X}^*)]_{ij} \geq 0$ according to the second condition in (4.1). Thus the condition (4.5) also holds for any $(i, j) \in \mathcal{I}_2$. Totally, the condition (4.5) holds. To sum up, all the KKT conditions (4.3)-(4.6) hold for any $\mathbf{X}^* \in \mathcal{M}^p$ satisfying the conditions in (4.1), and thus we can conclude that \mathbf{X}^* is the minimizer of Problem (2.1). \square

The convergence analysis of our algorithm needs the following assumption on the minimizer \mathbf{X}^* , which is equivalent to the strict complementary slackness condition. This assumption is mild because Theorem 4.1 shows that \mathbf{X}^* must satisfy $[\nabla f(\mathbf{X}^*)]_{ij} \leq 0$ for each $(i, j) \in \mathcal{V} \setminus \mathcal{E}$. We only need this inequality to be strict.

Assumption 4.2. For the minimizer \mathbf{X}^* of Problem (2.1), we assume that the gradient of the objective function f at \mathbf{X}^* satisfies

$$[\nabla f(\mathbf{X}^*)]_{ij} < 0, \quad \forall (i, j) \in \mathcal{V} \setminus \mathcal{E},$$

where $\mathcal{V} = \{(i, j) \in [p]^2 \mid [\mathbf{X}^*]_{ij} = 0\}$, and \mathcal{E} is the disconnectivity set.

Next we show that the sequence $\{\mathbf{X}_k\}$ generated by our algorithm converges to the minimizer \mathbf{X}^* , and the set \mathcal{I}_k^c exactly identifies the support of \mathbf{X}^* in a finite number of iterations. Our recent work [45] presented an initial exploration on second-order algorithms for graph learning with ℓ_1 -regularization under irrepresentability condition, which fails to establish convergence guarantees because of the discontinuity at boundary caused by the partitioning scheme and lack of a well-designed line search method.

THEOREM 4.3. *Under Assumption 4.2, the sequence $\{\mathbf{X}_k\}$ generated by Algorithm 3.1 converges to the minimizer \mathbf{X}^* of Problem (2.1), with $\{f(\mathbf{X}_k)\}$ monotonically decreasing. Moreover, there exists some $k_o \in \mathbb{N}_+$ such that*

$$\mathcal{I}_k^c = \text{supp}(\mathbf{X}_k) = \text{supp}(\mathbf{X}^*), \quad \forall k \geq k_o.$$

Proof. Following from Proposition 3.4, for any iterate $\mathbf{X}_k \in L_f$, a small enough step size ensures that the line search condition (3.25) holds, which leads to a sufficient decrease of the objective function as shown in Proposition 3.6, and the next iterate $\mathbf{X}_{k+1} \in L_f$. When the sequence starts with $\mathbf{X}_0 \in L_f$, each point of the sequence $\{\mathbf{X}_k\}_{k \geq 0}$ admits $\mathbf{X}_k \in L_f$. Note that it is easy to construct an initial point $\mathbf{X}_0 \in L_f$, because we could consider an $\mathbf{X}^o \in \mathcal{U}^p$ in (3.27), which is close to $\text{cl}(\mathcal{U}^p) \setminus \mathcal{U}^p$ such that $f(\mathbf{X}^o)$ sufficiently large, following from the fact that $f(\mathbf{X}) = +\infty$ for any $\mathbf{X} \in \text{cl}(\mathcal{U}^p) \setminus \mathcal{U}^p$. Lemma 3.5 shows that the lower level set L_f is compact, thus the sequence $\{\mathbf{X}_k\}$ has at least one limit point. For every limit \mathbf{X}^* of the sequence $\{\mathbf{X}_k\}$, we have $\mathbf{X}^* \in \mathcal{M}^p$. Define $\mathcal{I}^* = \mathcal{T}(\mathbf{X}^*, \epsilon^*) \cup \mathcal{E}$, where $\mathcal{T}(\mathbf{X}^*, \epsilon^*)$ is equal to

$$\mathcal{T}(\mathbf{X}^*, \epsilon^*) = \{(i, j) \in [p]^2 \mid -\epsilon^* \leq [\mathbf{X}^*]_{ij} \leq 0, [\nabla f(\mathbf{X}^*)]_{ij} < 0\},$$

and ϵ^* is defined as $\epsilon^* := \min(2(1-\alpha)m^2 \|\nabla f(\mathbf{X}^*)\|_{\mathcal{T}_\delta^* \setminus \mathcal{E}}, \delta)$, where \mathcal{T}_δ^* denotes $\mathcal{T}(\mathbf{X}^*, \delta)$. The line search condition (3.25) allows $\{f(\mathbf{X}_k)\}$ to keep decreasing until $[\mathbf{X}_k]_{\mathcal{I}_k} = \mathbf{0}$, and $[\nabla f(\mathbf{X}_k)]_{\mathcal{I}_k^c} = \mathbf{0}$. Therefore, every limit point \mathbf{X}^* must satisfy

$$(4.8) \quad [\mathbf{X}^*]_{\mathcal{I}^*} = \mathbf{0}, \quad \text{and} \quad [\nabla f(\mathbf{X}^*)]_{\{\mathcal{I}^*\}^c} = \mathbf{0}.$$

We show that every limit point \mathbf{X}^* is the minimizer of Problem (2.1) according to Theorem 4.1. Let $\mathcal{V} = \{(i, j) \in [p]^2 \mid [\mathbf{X}^*]_{ij} = 0\}$. First, for any $(i, j) \in \mathcal{E}$, we have $[\mathbf{X}^*]_{ij} = 0$, because of the projection \mathcal{P}_Ω in each iteration. Note that $[\mathbf{X}^*]_{ij} = 0$ for any $(i, j) \in \mathcal{I}^*$ according to (4.8). For any $(i, j) \in \mathcal{V}^c$, i.e., $[\mathbf{X}^*]_{ij} \neq 0$, we must have $(i, j) \in \{\mathcal{I}^*\}^c$. Together with (4.8), $[\nabla f(\mathbf{X}^*)]_{\mathcal{V}^c} = \mathbf{0}$ holds. For any $(i, j) \in \mathcal{V} \setminus \mathcal{E}$, we must have $(i, j) \in \mathcal{T}(\mathbf{X}^*, \epsilon^*) \cup \{\mathcal{I}^*\}^c$. Recall that $[\nabla f(\mathbf{X}^*)]_{ij} < 0$ for any $(i, j) \in \mathcal{T}(\mathbf{X}^*, \epsilon^*)$, and $[\nabla f(\mathbf{X}^*)]_{ij} = 0$ for any $(i, j) \in \{\mathcal{I}^*\}^c$. Overall, we obtain $[\nabla f(\mathbf{X}^*)]_{\mathcal{V} \setminus \mathcal{E}} \leq \mathbf{0}$. To sum up, all the conditions in Theorem 4.1 hold for every limit point \mathbf{X}^* , and thus every limit point is the minimizer of Problem (2.1).

Since the minimizer of Problem (2.1) is unique, we obtain that the limit point of the sequence $\{\mathbf{X}_k\}$ is also unique, and thus $\{\mathbf{X}_k\}$ is convergent. Therefore, we conclude that the sequence $\{\mathbf{X}_k\}$ converges to the unique minimizer of Problem (2.1). The monotone decreasing of the sequence $\{f(\mathbf{X}_k)\}$ can be established by Proposition 3.6.

Finally, we prove that the support of \mathbf{X}^* is consistent with the set \mathcal{I}_k^c for a sufficiently large k . Without loss of generality, we specify the constant δ in (3.12) as

$$(4.9) \quad \delta = \omega \min_{(i, j) \in \text{supp}(\mathbf{X}^*)} |[\mathbf{X}^*]_{ij}|,$$

where $\omega \in (0, 1)$ is a constant. Note that the sequence $\{\mathbf{X}_k\}$ converges to \mathbf{X}^* . Under Assumption 4.2 that $[\nabla f(\mathbf{X}^*)]_{ij}$ is strictly negative for any $(i, j) \in \text{supp}^c(\mathbf{X}^*) \setminus \mathcal{E}$, there must exist some $a > 0$ and $K_1 \in \mathbb{N}_+$ such that

$$(4.10) \quad [\nabla f(\mathbf{X}_k)]_{ij} < -\frac{a}{2(1-\alpha)m^2}, \quad \forall (i, j) \in \text{supp}^c(\mathbf{X}^*) \setminus \mathcal{E}$$

holds for any $k \geq K_1$, where $\alpha \in (0, 1)$ is a constant, and m is a positive constant defined in Lemma 3.5. We consider a neighbourhood of \mathbf{X}^* defined by

$$(4.11) \quad \mathcal{N}(\mathbf{X}^*; r) := \{\mathbf{X} \in \mathbb{R}^{p \times p} \mid \|\mathbf{X} - \mathbf{X}^*\|_{\text{F}} \leq r\},$$

where r is a positive constant defined as

$$(4.12) \quad r := \min \left(c \min_{(i,j) \in \text{supp}(\mathbf{X}^*)} |[\mathbf{X}^*]_{ij}|, a, \delta \right),$$

where $c < 1 - \omega$ is a positive constant. There must exist $K_2 \in \mathbb{N}_+$ such that $\mathbf{X}_k \in \mathcal{N}(\mathbf{X}^*; r)$ holds for any $k \geq K_2$. Take $K_o = \max(K_1, K_2)$. For any $k \geq K_o$ and $(i, j) \in \text{supp}(\mathbf{X}^*)$, one has

$$|[\mathbf{X}^*]_{ij} - [\mathbf{X}_k]_{ij}| \leq |[\mathbf{X}^*]_{ij} - [\mathbf{X}_k]_{ij}| \leq \|\mathbf{X}_k - \mathbf{X}^*\|_{\text{F}} \leq r,$$

Thus one can obtain, for any $k \geq K_o$,

$$(4.13) \quad |[\mathbf{X}_k]_{ij}| \geq \min_{(i,j) \in \text{supp}(\mathbf{X}^*)} |[\mathbf{X}^*]_{ij}| - r > \delta > 0, \quad \forall (i, j) \in \text{supp}(\mathbf{X}^*),$$

where the last inequality follows from (4.9) and (4.12). Recall that for any $(i, j) \in \mathcal{T}(\mathbf{X}_k, \delta)$, $|[\mathbf{X}_k]_{ij}| \leq \delta$. Then one has

$$(4.14) \quad \mathcal{T}(\mathbf{X}_k, \delta) \subseteq \text{supp}^c(\mathbf{X}^*).$$

Then the ϵ_k in (3.12) can be bounded by

$$(4.15) \quad \epsilon_k \geq \min \left(2(1 - \alpha)m^2 \|\nabla f(\mathbf{X}_k)\|_{\text{supp}^c(\mathbf{X}^*) \setminus \mathcal{E}} \|_{\min}, \delta \right) \geq \min(a, \delta),$$

where the first and second inequalities follow from (4.14) and (4.10), respectively. For any $k \geq K_o$ and $(i, j) \in \mathcal{T}(\mathbf{X}_k, \epsilon_k) \cup \mathcal{E}$, one has $|[\mathbf{X}_k]_{ij}| \leq \epsilon_k \leq \delta$. Thus we obtain

$$(4.16) \quad \mathcal{T}(\mathbf{X}_k, \epsilon_k) \cup \mathcal{E} \subseteq \text{supp}^c(\mathbf{X}^*).$$

On the other hand, for any $k \geq K_o$ and $(i, j) \in \text{supp}^c(\mathbf{X}^*)$, one has

$$(4.17) \quad |[\mathbf{X}_k]_{ij}| = |[\mathbf{X}_k]_{ij} - [\mathbf{X}^*]_{ij}| \leq \|\mathbf{X}_k - \mathbf{X}^*\|_{\text{F}} \leq r \leq \epsilon_k,$$

where the last inequality follows from (4.12) and (4.15). Therefore, one has

$$\text{supp}^c(\mathbf{X}^*) \subseteq \mathcal{T}(\mathbf{X}_k, \epsilon_k) \cup \mathcal{E} \cup \mathcal{B}_k^{(1)} \cup \mathcal{B}_k^{(2)}.$$

Note that $\mathcal{B}_k^{(5)} \cap \text{supp}^c(\mathbf{X}^*) = \emptyset$, because any $(i, j) \in \mathcal{B}_k^{(5)}$ corresponds to the element on the diagonal which must be nonzero. Moreover, following from (4.10), one has

$$(\text{supp}^c(\mathbf{X}^*) \setminus \mathcal{E}) \cap \mathcal{B}_k^{(1)} = \emptyset, \quad \text{and} \quad (\text{supp}^c(\mathbf{X}^*) \setminus \mathcal{E}) \cap \mathcal{B}_k^{(2)} = \emptyset.$$

Therefore, we can obtain $\text{supp}^c(\mathbf{X}^*) \subseteq \mathcal{T}(\mathbf{X}_k, \epsilon_k) \cup \mathcal{E}$. Together with (4.16), we obtain

$$(4.18) \quad \text{supp}^c(\mathbf{X}^*) = \mathcal{T}(\mathbf{X}_k, \epsilon_k) \cup \mathcal{E} = \mathcal{I}_k.$$

Equivalently, we have

$$(4.19) \quad \text{supp}(\mathbf{X}^*) = \mathcal{I}_k^c, \quad \forall k \geq K_o.$$

We can see that the sets \mathcal{I}_k and \mathcal{I}_k^c are fixed for any $k \geq K_o$. Therefore, following from the iterate of \mathbf{X}_{k+1} , $[\mathbf{X}_{k+1}]_{\mathcal{I}_{k+1}} = [\mathbf{X}_{k+1}]_{\mathcal{I}_k} = \mathbf{0}$ for any $k \geq K_o$. Moreover, together with (4.13) and (4.19), we obtain that for any $k \geq K_o$, $[\mathbf{X}_{k+1}]_{\mathcal{I}_{k+1}^c} \neq \mathbf{0}$. Take $k_o = K_o + 1$. We obtain $\text{supp}(\mathbf{X}_k) = \mathcal{I}_k^c$ for any $k \geq k_o$, completing the proof. \square

In what follows, we discuss the convergence rate of our algorithm. Following from Theorem 4.3, the support of \mathbf{X}_k is fixed and consistent with that of the minimizer for any $k \geq k_o$. As a result, iterate (3.23) of our algorithm over \mathcal{I}_k^c can be written as

$$(4.20) \quad [\mathbf{X}_{k+1}]_{\mathcal{I}_k^c} = [\mathbf{X}_k]_{\mathcal{I}_k^c} - \gamma_k \mathbf{R}_k^{-1} [\nabla f(\mathbf{X}_k)]_{\mathcal{I}_k^c},$$

where $\mathbf{R}_k^{-1} = [\mathbf{H}_k^{-1}]_{\mathcal{I}_k^c \mathcal{I}_k^c}$ is the scaling matrix, which is positive definite and admits

$$(4.21) \quad \mathbf{R}_k = [\mathbf{H}_k]_{\mathcal{I}_k^c \mathcal{I}_k^c} - [\mathbf{H}_k]_{\mathcal{I}_k^c \mathcal{I}_k} [\mathbf{H}_k]_{\mathcal{I}_k \mathcal{I}_k}^{-1} [\mathbf{H}_k]_{\mathcal{I}_k^c \mathcal{I}_k}^{\top}.$$

Define m_k and M_k as the smallest and largest eigenvalues of $\mathbf{R}_k^{-\frac{1}{2}} [\mathbf{H}_k]_{\mathcal{I}_k^c \mathcal{I}_k^c} \mathbf{R}_k^{-\frac{1}{2}}$, respectively. The following theorem shows that the convergence rate depends on the condition number m_k/M_k of $\mathbf{R}_k^{-\frac{1}{2}} [\mathbf{H}_k]_{\mathcal{I}_k^c \mathcal{I}_k^c} \mathbf{R}_k^{-\frac{1}{2}}$. If we replace the matrix \mathbf{R}_k by an identity matrix, (*i.e.*, turn the iterate into the projected gradient method), then the convergence rate will depend on the condition number of $[\mathbf{H}_k]_{\mathcal{I}_k^c \mathcal{I}_k^c}$. We note that the condition number of $\mathbf{R}_k^{-\frac{1}{2}} [\mathbf{H}_k]_{\mathcal{I}_k^c \mathcal{I}_k^c} \mathbf{R}_k^{-\frac{1}{2}}$ could be larger than that of $[\mathbf{H}_k]_{\mathcal{I}_k^c \mathcal{I}_k^c}$, since \mathbf{R}_k could approximate $[\mathbf{H}_k]_{\mathcal{I}_k^c \mathcal{I}_k^c}$ well. Therefore, the gradient scaling matrix \mathbf{R}_k^{-1} , *i.e.*, $[\mathbf{H}_k^{-1}]_{\mathcal{I}_k^c \mathcal{I}_k^c}$, leads our algorithm to converge faster than the projected gradient method, while they require the same orders of computation and memory costs.

THEOREM 4.4. *Under Assumption 4.2, the sequence $\{\mathbf{X}_k\}$ generated by Algorithm 3.1 satisfies*

$$\limsup_{k \rightarrow \infty} \frac{\|\mathbf{X}_{k+1} - \mathbf{X}^*\|_{\mathbf{M}_k}^2}{\|\mathbf{X}_k - \mathbf{X}^*\|_{\mathbf{M}_k}^2} \leq \limsup_{k \rightarrow \infty} \left(1 - \min \left(m_k, \frac{2(1-\alpha)\beta m_k}{M_k} \right) \right)^2.$$

Proof. Theorem 4.4 is a direct extension of the result in [7]. Let g be twice continuously differentiable and consider the following iterate

$$\mathbf{x}_{x+1} = \mathbf{x}_k - \gamma_k \mathbf{D}_k \nabla g(\mathbf{x}_k),$$

where \mathbf{D}_k is positive definite and symmetric. Then the sequence $\{\mathbf{x}_k\}$ admits the following convergence result [7],

$$(4.22) \quad \limsup_{k \rightarrow \infty} \frac{\|\mathbf{x}_{k+1} - \mathbf{x}^*\|_{\mathbf{D}_k^{-1}}^2}{\|\mathbf{x}_k - \mathbf{x}^*\|_{\mathbf{D}_k^{-1}}^2} = \limsup_{k \rightarrow \infty} \max \left(|1 - \gamma_k m'_k|^2, |1 - \gamma_k M'_k|^2 \right),$$

where \mathbf{x}^* is the limit of the sequence $\{\mathbf{x}_k\}$, which satisfies that $\nabla g(\mathbf{x}^*) = \mathbf{0}$ and $\nabla^2 g(\mathbf{x}^*)$ is positive definite, and m'_k and M'_k are the smallest and largest eigenvalues of $(\mathbf{D}_k)^{1/2} \nabla^2 g(\mathbf{x}_k) (\mathbf{D}_k)^{1/2}$, respectively. This conclusion is extended from the convergence result for the quadratic objective function. Conceptually, this makes sense because a twice continuously differentiable objective function is very close to a positive definite quadratic function in the neighborhood of a non-singular local minimum.

Following from Theorem 4.3, for any $k \geq k_o$, iterate (3.23) can be written as iterate (4.20), which reduces to an iterate of an unconstrained optimization algorithm on some subspace. Following from the results in (4.22), we obtain

$$(4.23) \quad \limsup_{k \rightarrow \infty} \frac{\|[\mathbf{X}_{k+1}]_{\mathcal{I}_k^c} - [\mathbf{X}^*]_{\mathcal{I}_k^c}\|_{\mathbf{R}_k}^2}{\|[\mathbf{X}_k]_{\mathcal{I}_k^c} - [\mathbf{X}^*]_{\mathcal{I}_k^c}\|_{\mathbf{R}_k}^2} = \limsup_{k \rightarrow \infty} \max \left(|1 - \gamma_k m_k|^2, |1 - \gamma_k M_k|^2 \right),$$

where m_k and M_k are the smallest and largest eigenvalues of $\mathbf{R}_k^{-\frac{1}{2}} [\mathbf{H}_k]_{\mathcal{I}_k^c \mathcal{I}_k^c} \mathbf{R}_k^{-\frac{1}{2}}$, respectively. Following from (3.16), Theorem 4.3, and $\mathbf{R}_k^{-1} = [\mathbf{H}_k^{-1}]_{\mathcal{I}_k^c \mathcal{I}_k^c}$, we obtain

$$(4.24) \quad \|[\mathbf{X}_k]_{\mathcal{I}_k^c} - [\mathbf{X}^*]_{\mathcal{I}_k^c}\|_{\mathbf{R}_k}^2 = \|\mathbf{X}_k - \mathbf{X}^*\|_{\mathbf{M}_k}^2, \quad \forall k \geq k_o.$$

When $k \geq k_o$, the line search condition reduces to

$$f(\mathbf{X}_{k+1}) \leq f(\mathbf{X}_k) - \alpha \gamma_k \langle [\nabla f(\mathbf{X}_k)]_{\mathcal{I}_k^c}, [\mathbf{P}_k]_{\mathcal{I}_k^c} \rangle.$$

Similar to the unconstrained case in [5], the step size must satisfy the line search condition if $\gamma_k \geq \min(1, 2(1 - \alpha)\beta/M_k)$ as $k \rightarrow \infty$. Then together with (4.23) and (4.24), we complete the proof. \square

5. Experimental Results. We conduct experiments on synthetic and real-world data to verify the performance of the proposed algorithm. All experiments were conducted on 2.10GHZ Xeon Gold 6152 machines with 80G RAM and Linux OS, and all compared methods were implemented in MATLAB.

The state-of-the-art methods for comparing the computational time in estimating sparse precision matrices under MTP_2 constraints include:

- **BCD:** block coordinate descent algorithm proposed in [41], which updates a single column/row of the precision matrix at a time by solving a nonnegative quadratic program on the primal variable.
- **optGL:** block coordinate descent algorithm proposed in [34], which solves nonnegative quadratic programs on the dual variable.
- **GGL:** block coordinate descent algorithm proposed in [13], which solves nonnegative quadratic programs on the primal variable similar to BCD, but can handle disconnectivity constraints.
- **PGD:** projected gradient descent method with the backtracking line search, which is a baseline method. The iterate is formulated in (3.2).
- **APGD:** accelerated projected gradient algorithm [31] that employs an extrapolation step.
- **PQN-LBFGS:** projected quasi-Newton method that employs the limited-memory BFGS to approximate the inverse Hessian [22].

Note that all the state-of-the-art methods listed above can converge to the minimizer of Problem (2.1), and we focus on the comparisons of the computational time required for those methods. To that end, we report the relative error of the objective function value as a function of the run time, which is calculated by

$$(5.1) \quad |f(\mathbf{X}_k) - f(\mathbf{X}^*)| / |f(\mathbf{X}^*)|,$$

where f is the objective function of Problem (2.1), and \mathbf{X}^* is its minimizer. The \mathbf{X}^* is computed by running the state-of-the-art method **GGL** [13] until it converges to a

point $\mathbf{X}_k \in \mathcal{M}^p$ satisfying

$$(5.2) \quad [\mathbf{X}_k]_{ij} = 0 \quad \forall (i, j) \in \mathcal{E}, \quad [\nabla f(\mathbf{X}_k)]_{\mathcal{A} \setminus \mathcal{E}} \leq \mathbf{0}, \quad \text{and} \quad \|[\nabla f(\mathbf{X}^*)]_{\mathcal{A}^c}\|_{\max} \leq 10^{-8},$$

where $\mathcal{A} := \{(i, j) \in [p]^2 \mid |[\mathbf{X}_k]_{ij}| \leq 10^{-8}\}$. Through the comparison with the sufficient and necessary conditions of the unique minimizer of Problem (2.1) presented in Theorem 4.1, we can see that any point \mathbf{X}_k satisfying the conditions (5.2) is very close to the minimizer. There is no additional computational cost for PGD, APGD, PQN-LBFGS and our proposed FPN in computing the relative error as shown in (5.1), because the objective function value has been evaluated in the backtracking line search in each iteration. The methods BCD, optGL, and GGL do not need to evaluate the objective function, and thus additional cost is needed in computing the relative error in (5.1) for comparisons. However, this cost can be almost ignored, since they compute the objective function value only after completing a cycle, and the number of cycles required for BCD, optGL, and GGL is considerably smaller than the number of iterations required for the other methods.

We set the regularization parameter λ_{ij} in Problem (2.1) as follows

$$(5.3) \quad \lambda_{ij} = \frac{\sigma}{|[\hat{\mathbf{X}}]_{ij}| + \epsilon}, \quad \forall i \neq j,$$

where $\hat{\mathbf{X}}$ is some estimator, ϵ is set as 10^{-3} , and $\sigma > 0$ is the parameter to adjust the sparsity. The function in (5.3) is closely related to the re-weighted ℓ_1 -norm regularization [8, 23], which is effective in enhancing the sparsity of the solution. We use the maximum likelihood estimator as $\hat{\mathbf{X}}$, *i.e.*, the minimizer of Problem (2.1) without the sparsity regularization. Note that one may solve the maximum likelihood estimator with a relatively large tolerance to obtain a coarse estimator, and one may also explore other monotonically decreasing functions in (5.3). For PQN-LBFGS, we use the previous 50 updates to compute the search direction. For our proposed FPN, we set $\epsilon_k = 10^{-15}$ in (3.11) for identifying the set of *restricted* variables.

5.1. Synthetic Data. We generate independent samples $\mathbf{y}^{(1)}, \dots, \mathbf{y}^{(n)} \in \mathbb{R}^p$ from a multivariate Gaussian distribution with zero mean and precision matrix Θ , where $\Theta \in \mathcal{M}^p$ is the underlying precision matrix associated with a graph consisting of p nodes. Then the sample covariance matrix is constructed by $\mathbf{S} = \frac{1}{n} \sum_{i=1}^n \mathbf{y}^{(i)} (\mathbf{y}^{(i)})^\top$.

We consider Barabasi-Albert (BA) graphs [3] as the model for the support of the underlying precision matrix. BA models play an important role in network science, which generate random scale-free networks using a *preferential attachment* mechanism such that new nodes tend to link to nodes that have higher degree in the evolution. Scale-free networks are well-suited to model the Internet, protein interaction networks, citation networks, and most social and online networks [3]. A BA graph of degree r indicates that each new node is connected to r existing nodes with a probability that is proportional to the number of edges that the existing nodes already have. The illustration of BA graphs can be found in appendix.

We adopt the procedures used in [41] to generate the underlying precision matrix Θ . We first set

$$(5.4) \quad \tilde{\Theta} = \delta \mathbf{I} - \mathbf{A}, \quad \text{with} \quad \delta = 1.05 \lambda_{\max}(\mathbf{A}),$$

where $\lambda_{\max}(\mathbf{A})$ denotes the largest eigenvalue of \mathbf{A} , and \mathbf{A} contains all the graph weights, in which the weight is zero if two nodes are disconnected, and follows a uniform distribution $U(2, 5)$ otherwise. Finally, we set $\Theta = \mathbf{D} \tilde{\Theta} \mathbf{D}$, where \mathbf{D} is a diagonal matrix chosen such that the covariance matrix Θ^{-1} has unit diagonal elements.

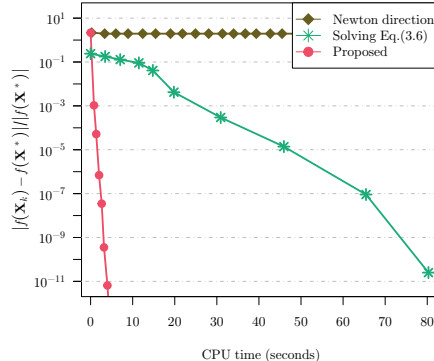


Fig. 1: Comparisons of convergence of the proposed algorithm, the algorithm that solves a sequence of the convex approximation problems in (3.6), and the algorithm that uses the Newton direction from Lemma 3.2.

5.1.1. Comparisons of convergence. We compare the convergence of algorithms using different search directions. Figure 1 shows that our algorithm using the direction from Lemma 3.3 converges to the minimizer, which is consistent with our theoretical convergence results presented in Theorem 4.3.

In contrast, the objective function value of the algorithm using the direction from Lemma 3.2 in iterate (3.8) does not continue decreasing after a few iterations. Note that the algorithm selects the step size by the Armijo rule, *i.e.*, the step size is repeatedly reduced until the next iterate leads to a decrease of the objective function. Therefore, the Newton direction from Lemma 3.2 cannot decrease the objective function value for any positive step size, implying that it cannot be guaranteed to be a descent direction. Figure 1 also compares with the convergence of the algorithm which solves a sequence of the convex approximation problems in (3.6). It is observed in Figure 1 that this method converges to the optimal solution, while it takes significantly more time than our proposed algorithm for convergence. Since the problem in (3.6) cannot be solved by the widely used `quadprog` solver because of the huge memory consumption, we solve this problem via the projected gradient descent method.

5.1.2. Comparisons of computational time. We compare the computational time of our algorithm with the state-of-the-art methods on synthetic data sets. All results are averaged over 10 realizations. The regularization parameter σ in (5.3) is chosen such that the minimizer has a close number of nonzero elements as compared to that of the underlying precision matrix. We plot markers at every 10 iterations for PGD, APGD, PQN-LBFGS, and FPN, whereas we plot a marker for each cycle of updating all columns/rows for the BCD-type algorithms BCD, GGL, and `optGL`.

Figure 2 compares the computational time of different methods in solving Problem (2.1) on BA graphs of degree one. It is observed that our proposed FPN takes significantly less time than all state-of-the-art methods to converge to the minimizer for the number of nodes ranging from 1000 to 5000. We also observe that the methods BCD and GGL are efficient for the cases of 1000 nodes, where they are faster than PGD and APGD, and competitive with PQN-LBFGS. However, as the number of nodes p increases to 5000, BCD and GGL become slower than PGD, APGD and PQN-LBFGS. This is because BCD and GGL require $O(p^4)$ operations in each cycle for solving p nonnegative quadratic programs, where the computational cost grows quickly with the increase of p . The `optGL` empirically requires fewer cycles than BCD and GGL for convergence, while the former costs much more time in each cycle than the latter.

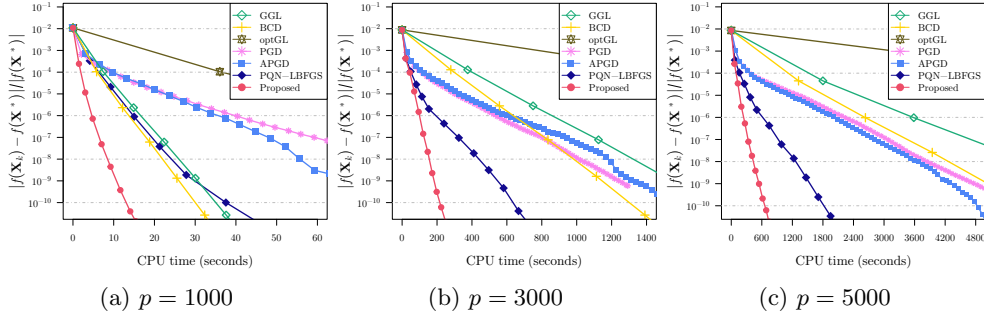


Fig. 2: Relative errors of the objective function values versus time on BA graphs of degree one consisting of p nodes: (a) $p = 1000$, (b) $p = 3000$, and (c) $p = 5000$.

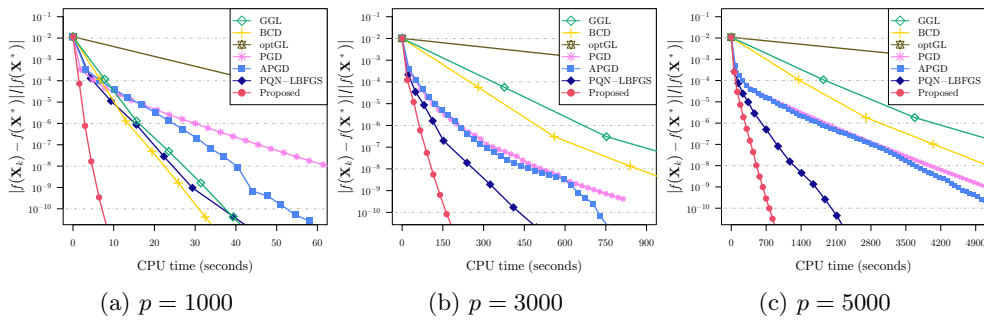


Fig. 3: Relative errors of the objective function value versus time on BA graphs of degree two consisting of p nodes: (a) $p = 1000$, (b) $p = 3000$, and (c) $p = 5000$.

Figure 3 presents the computational time of different algorithms in solving Problem (2.1) on BA graphs of degree two. Similar to the conclusions made on BA graphs of degree one, we observe that FPN is significantly more efficient than the state-of-the-art methods in terms of computational time for different numbers of nodes. We also observe that PQN-LBFGS and FPN take less iterations to converge to the minimizer than PGD and APGD, especially when the dimension is very high (*e.g.*, $p = 5000$), indicating that the former converge faster than the latter. This is because both PQN-LBFGS and FPN exploit the second-order information and use the approximate Newton direction as the search direction, which is useful to overcome the issue of low convergence rate arising from first-order methods in high-dimensional cases.

Figure 4 compares the computational time of different algorithms in solving Problem (2.1) for the case that a disconnectivity set is imposed. We observe that the proposed FPN always costs the least time to converge to the minimizer. We do not compare with BCD and optGL, because they cannot handle the disconnectivity constraint. PQN-LBFGS originally does not aim to solve the problem with the disconnectivity constraint, thus we update the projection and the construction of the set of *fixed* variables based on our proposed method such that it can handle the disconnectivity constraint.

Figure 5 evaluates the impact of different values of the regularization parameter σ in (5.3) on the run time for each algorithm. We observe that the run time of BCD, GGL and FPN remain stable for different values of σ , while the run time of other methods grows as σ decreases. Thus, BCD, GGL and FPN are more robust against the setting of the regularization parameter in terms of the run time. In our experiments,

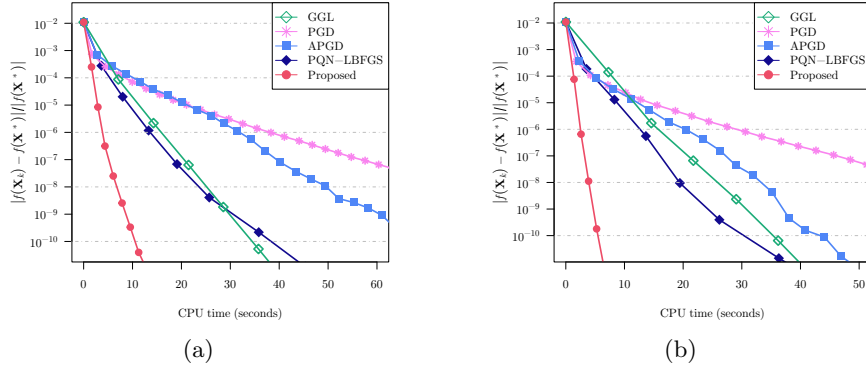


Fig. 4: Relative errors of the objective function values versus time in solving Problem (2.1) on data sets: (a) BA graphs of degree one and (b) BA graphs of degree two, with imposing 1% disconnectivities. The disconnectivity set \mathcal{E} in Problem (2.1) is constructed by randomly collecting 1% of the indexes corresponding to the zero elements of the underlying precision matrix Θ . Both the graphs consist of 1000 nodes.

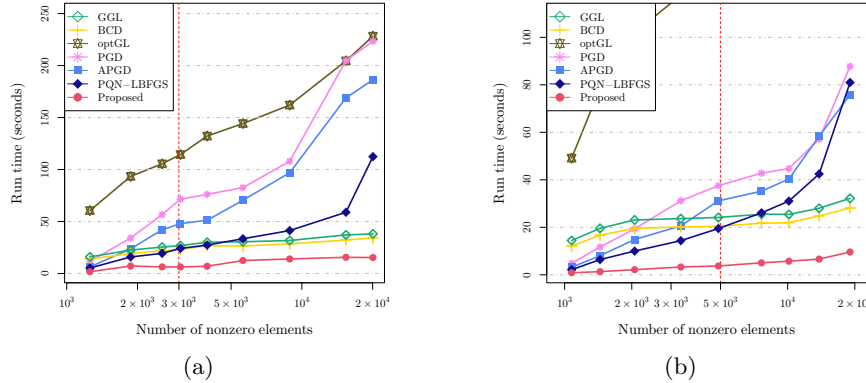


Fig. 5: Run time versus numbers of nonzero elements of the estimated precision matrices under different values of the regularization parameter on data sets: (a) BA graph of degree one and (b) BA graph of degree two, both consisting of 1000 nodes, where the underlying precision matrices have 2998 and 4994 nonzero elements (indicated by the vertical red lines), respectively.

σ takes a sequence of values from 0.02 to 0.0015 to adjust the sparsity level. Each algorithm terminates when it achieves $|f(\mathbf{X}_k) - f(\mathbf{X}^*)|/|f(\mathbf{X}^*)| < 10^{-7}$.

5.2. Real-world data. We conduct experiments on two real-world data sets: *concepts* data set and financial time-series data set. On the *concepts* data set, we compare the computational time of different algorithms for solving Problem (2.1). On the financial time-series data set, we present the performance of our method on the graph edge recovery.

5.2.1. Concepts Data. The *concepts* data set [24], collected by Intel Labs, includes 1000 nodes and 218 semantic features, *i.e.*, $p = 1000$ and $n = 218$. Each node denotes a concept such as “house”, “coat”, and “whale”, and each semantic feature is a question such as “Can it fly?”, “Is it alive?”, and “Can you use it?”. The answers are on a five-point scale from “definitely no” to “definitely yes”, conducted on Amazon Mechanical Turk.

Figure 6 compares the run time of different algorithms for solving Problem (2.1) on the *concepts* data. We observe that our proposed FPN requires significantly less time to converge to the minimizer than the state-of-the-art algorithms, which is consistent with the observations in synthetic experiments. Note that all the compared algorithms can converge to the minimizer of Problem (2.1), and thus learn the same graph.

Figure 7 presents a connected subgraph illustrated by the minimizer of Problem (2.1). Interestingly, it is observed that the learned graph builds a semantic network, where the nodes with related concepts are more closely connected. For example, the concepts related to insects like “bee”, “butterfly”, “flea”, “mosquito”, and “spider” are grouped together, while the concepts related to human such as “baby”, “husband”, “child”, “girls”, and “man” form another group. Moreover, the network shown in Figure 7 connects “penguin” closely to birds like “owl” and “crow”, as well as sea animals like “goldfish” and “seal”, reflecting it as an aquatic bird. To conclude, the learned network can characterize the relationships between concepts well.

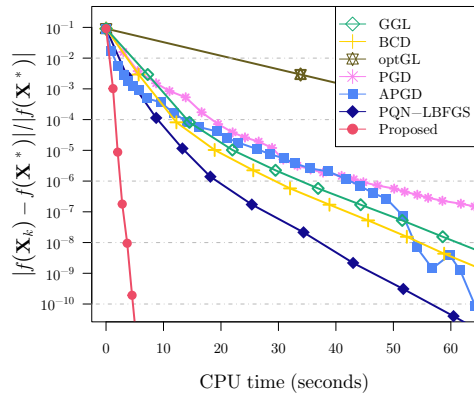


Fig. 6: Relative errors of the objective function values versus time for different algorithms in solving Problem (2.1) on the *concepts* data set, consisting of 1000 nodes.

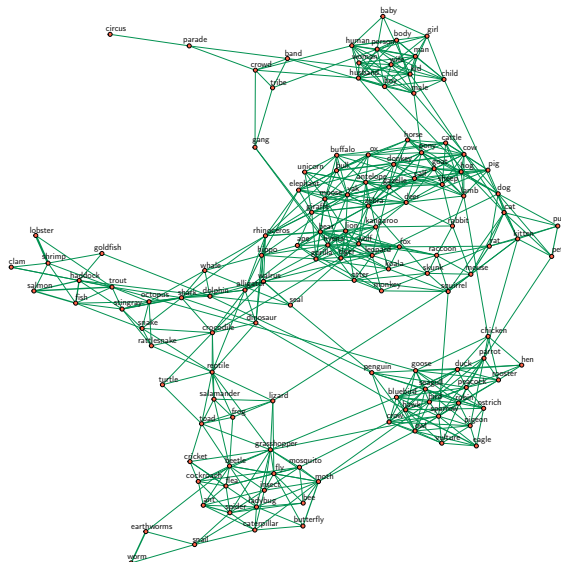


Fig. 7: The connected subgraph illustrated by the minimizer \mathbf{X}^* of Problem (2.1) on the *concepts* data set, which consists of 132 nodes.

5.2.2. Financial Time-series Data. We conduct numerical experiments on the financial time-series data set to verify the performance of our method on graph edge recovery. MTP₂ models are justified well on financial time-series data since the market factor leads to positive dependencies among stocks [1]. The data is collected from 201 stocks composing the S&P 500 index during the period from Jan. 1st 2017 to Jan. 1st 2020, resulting in 753 observations per stock, *i.e.*, $p = 201$ and $n = 753$. We construct the log-returns data matrix by $X_{i,j} = \log P_{i,j} - \log P_{i-1,j}$, where $P_{i,j}$ denotes the closing price of the j -th stock on the i -th day. The stocks are categorized into 5 sectors by the global industry classification standard system: Consumer Staples, Utilities, Industrials, Information Technology, and Energy.

We cannot directly assess whether the learned graph edges are correct because the underlying graph structure is unknown in the financial time-series data. Since we expect stocks belonging to the same sector to be linked together, we use the *modularity* [32] to measure the performance of edge recovery. Given a graph $\mathcal{G} = (V, E)$, where V is the vertex set and E is the edge set, the *modularity* is defined by

$$(5.5) \quad Q := \frac{1}{2|E|} \sum_{i,j \in V} \left(A_{ij} - \frac{d_i d_j}{2|E|} \right) \delta(c_i, c_j),$$

where $A_{ij} = 1$ if $(i, j) \in E$, and 0 otherwise, d_i denotes the number of edges of node i , c_i denotes the type of node i , and $\delta(c_i, c_j) = 1$ if $c_i = c_j$ and 0 otherwise. A stock graph with a high *modularity* value has dense connections between stocks within the same sector, and has sparse connections between stocks in distinct sectors. A higher *modularity* indicates a better representation of the actual network of stocks.

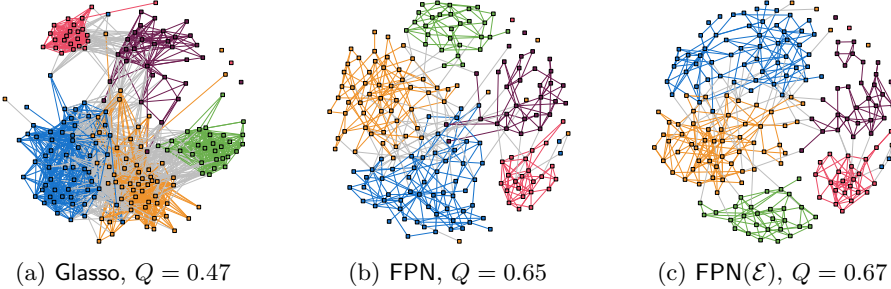


Fig. 8: Financial time-series graphs learned via (a) Glasso, (b) FPN, and (c) FPN(\mathcal{E}).

Figure 8 presents that the performances of FPN and FPN(\mathcal{E}) are better than that of Glasso [15], since most connections in the graphs learned via FPN and FPN(\mathcal{E}) are between nodes within the same sector, while only few connections (gray-colored edges) exist between nodes from distinct sectors. FPN and FPN(\mathcal{E}) achieve higher *modularity* values than Glasso, indicating that the former have a higher degree of interpretability than the latter. We also observe that FPN(\mathcal{E}) improves the performance of FPN in a moderate way. We fine-tune the sparsity regularization parameter for each method based on the *modularity* value while allowing only a few isolated nodes. FPN(\mathcal{E}) refers to using FPN to solve Problem (2.1) imposing a disconnectivity set \mathcal{E} which is obtained by conducting the hard thresholding on the MLE that is also used in computing regularization weights in (5.3). Numerical results in Figure 8 show that our method can potentially identify the underlying graph edges. In fact, we can prove that our method can exactly identify the edges of the underlying graph given enough observations that are sampled from an MTP₂ Gaussian distribution (please refer to the theory and proof in appendix for interests).

6. Conclusions. In this paper, we have proposed a fast projected Newton-like method for estimating precision matrices under MTP_2 constraints. Our algorithm only requires the same orders of computation and memory costs as those of the projected gradient method. The theoretical convergence analysis have been established. Extensive experiments have demonstrated that our algorithm is significantly more efficient than the state-of-the-art methods in terms of computational time. We have applied our method in financial time-series data, and observed a significant performance in terms of *modularity* value on the learned financial networks.

Appendix A. Additional results on support recovery consistency. In this section, we establish the support recovery consistency of our method to show that our method can exactly identify the edges of the underlying graph given enough observations.

We start by the notation and assumption needed for establishing theoretical results. Let $\Theta \in \mathcal{M}^p$ be the underlying precision matrix, whose support set $\text{supp}(\Theta)$ is

$$\mathcal{S} := \{(i, j) \in [p]^2 \mid \Theta_{ij} \neq 0\}.$$

The support set can be partitioned into two disjoint subsets, the indexes corresponding to the elements on the diagonal and off the diagonal, *i.e.*, $\mathcal{S} = \mathcal{S}_{\text{on}} \cup \mathcal{S}_{\text{off}}$, where

$$\mathcal{S}_{\text{on}} := \{(i, j) \in [p]^2 \mid \Theta_{ij} > 0, i = j\}, \text{ and } \mathcal{S}_{\text{off}} := \{(i, j) \in [p]^2 \mid \Theta_{ij} < 0, i \neq j\}.$$

Note that all the off-diagonal elements of Θ are nonpositive, and the elements on the diagonal are strictly positive, due to the fact that $\Theta \in \mathcal{M}^p$. Then we define

$$\mathcal{S}^c := \{(i, j) \in [p]^2 \mid \Theta_{ij} = 0\},$$

where all indexes in \mathcal{S}^c correspond to the off-diagonal elements. Let

$$\mathcal{S}' = \mathcal{S}^c \setminus \mathcal{E},$$

where \mathcal{E} is the disconnectivity set imposed in Problem (2.1), and we assume $\mathcal{E} \subseteq \mathcal{S}^c$.

Let d be the maximum number of nonzero elements in any row of Θ , which corresponds to the maximum degree of the underlying graph. Note that we include the diagonal elements of Θ when counting the degree, which can be viewed as the self-loop of each node.

We define two quantities that only depend on the underlying precision matrix,

$$(A.1) \quad K_{\Sigma} = \max_{i \in [p]} \sum_{j=1}^p |\Sigma_{ij}|, \quad \text{and} \quad K_H = \left\| (\mathbf{H}_{\mathcal{S}\mathcal{S}})^{-1} \right\|_{\infty},$$

where Σ is the underlying covariance matrix, *i.e.*, $\Sigma = \Theta^{-1}$, and $\mathbf{H}_{\mathcal{S}\mathcal{S}}$ is a $|\mathcal{S}| \times |\mathcal{S}|$ principle submatrix of \mathbf{H} , with both rows and columns indexed by \mathcal{S} , in which \mathbf{H} is the Hessian matrix at Θ , *i.e.*, $\mathbf{H} = \Theta^{-1} \otimes \Theta^{-1}$. $\|\mathbf{X}\|_{\infty}$ denotes the $\ell_{\infty}/\ell_{\infty}$ -operator norm given by $\|\mathbf{X}\|_{\infty} := \max_{i=1, \dots, p} \sum_{j=1}^p |X_{ij}|$.

We collect the regularization weights λ_{ij} , $(i, j) \in [p]^2$, of Problem (2.1) into a matrix $\boldsymbol{\lambda} \in \mathbb{R}^{p \times p}$. If we specify each weight as $\lambda_{ij} = C_{ij} \sqrt{\frac{\log p}{n}}$, then we have $\boldsymbol{\lambda} = \sqrt{\frac{\log p}{n}} \mathbf{C}$, where \mathbf{C} contains all the parameters C_{ij} . Note that we do not impose the sparsity penalty on the diagonal elements of \mathbf{X} , therefore $C_{ij} = 0$ for any $i = j$.

Let $\boldsymbol{\lambda}_{\mathcal{S}}$ denote the vector with the dimension $|\mathcal{S}|$ which contains the elements of $\boldsymbol{\Theta}$ indexed by \mathcal{S} .

Assumption A.1. The nonzero off-diagonal elements of $\boldsymbol{\Theta}$ satisfies

$$\min_{(i,j) \in \mathcal{S}_{\text{off}}} |\Theta_{ij}| > \frac{4}{3} K_H \|\boldsymbol{\lambda}_{\mathcal{S}}\|_{\max},$$

where $\|\boldsymbol{\lambda}_{\mathcal{S}}\|_{\max} = \max_{(i,j) \in \mathcal{S}} |\lambda_{ij}|$, in which λ_{ij} is the regularization weight.

Assumption A.1 imposes a lower bound on the minimal absolute value of $\boldsymbol{\Theta}$ over the set \mathcal{S}_{off} . This condition is mild because the regularization weight λ_{ij} in our theorem is taken with the order $\sqrt{\log p/n}$ that can be very small when the sample size n increases.

THEOREM A.2. *Suppose the regularization weights in Problem (2.1) are specified as $\boldsymbol{\lambda} = \sqrt{\frac{\log p}{n}} \mathbf{C}$ and satisfy*

$$(A.2) \quad \frac{\|\mathbf{C}_{\mathcal{S}'}\|_{\min}}{\|\mathbf{C}_{\mathcal{S}}\|_{\max}} \geq 2 \left\| \mathbf{H}_{\mathcal{S}'\mathcal{S}} (\mathbf{H}_{\mathcal{S}\mathcal{S}})^{-1} \right\|_{\infty},$$

and the sample covariance matrix \mathbf{S} satisfies

$$(A.3) \quad \|\boldsymbol{\Sigma} - \mathbf{S}\|_{\max} \leq c_0 \sqrt{\frac{\log p}{n}}.$$

Under Assumption A.1, if the sample size is lower bounded by $n \geq cd^2 \log p$, where $c = (4c_1 K_H K_{\Sigma} \max(4c_2 K_H K_{\Sigma}^2, 1))^2$, then the minimizer \mathbf{X}^* of Problem (2.1) recovers the support of the underlying precision matrix $\boldsymbol{\Theta}$ correctly, i.e.,

$$\text{supp}(\mathbf{X}^*) = \text{supp}(\boldsymbol{\Theta}),$$

where $c_0 = \frac{1}{6} \min(\|\mathbf{C}_{\mathcal{S}}\|_{\max}, \|\mathbf{C}_{\mathcal{S}'}\|_{\min})$, $c_1 = \|\mathbf{C}_{\mathcal{S}}\|_{\max}$, and $c_2 = \max\left(\frac{\|\mathbf{C}_{\mathcal{S}}\|_{\max}}{\|\mathbf{C}_{\mathcal{S}'}\|_{\min}}, 1\right)$.

Theorem A.2, proved in Appendix C, establishes the support recovery consistency of our method with the weighted ℓ_1 -norm in Problem (2.1), indicating that all the underlying graph edges associated with $\boldsymbol{\Theta}$ can be identified correctly. We note that the deviation condition (A.3) holds with an overwhelming probability $1 - k_1 \exp(-k_2 \log p)$ for Gaussian observations, or the more general class of sub-Gaussian observations, where k_1 and k_2 are two positive constants. If we view the quantities K_H and K_{Σ} as constants, then the requirement on the sample size is $n \gtrsim d^2 \log p$, which has only logarithmic dependence on the number of nodes p . For functions $h(n)$ and $g(n)$, we use $h(n) \gtrsim g(n)$ if $h(n) \geq cg(n)$, for some constant $c \in (0, +\infty)$.

Condition (A.2) depends on the parameters \mathbf{C} of the regularization weights. If some element Θ_{ij} of the underlying precision matrix is small or zero, then C_{ij} is expected to be large so as to impose a strong sparsity penalty on X_{ij} ; otherwise, C_{ij} is expected to be small. Therefore, we compute \mathbf{C} in an adaptive way based on an initial estimator \mathbf{X}_o . We consider

$$(A.4) \quad C_{ij} = \psi(|[\mathbf{X}_o]_{ij}|), \quad \forall i \neq j,$$

where ψ is a monotonically decreasing function. For example, $\psi(x) = (x + \epsilon)^{-1}$, in which ϵ is a small positive scalar. We may consider the maximum likelihood estimator as \mathbf{X}_o , which is a consistent estimator and exists with only two observations. As

the number of samples grows, $[\mathbf{X}_o]_{ij}$ will converge to zero for any $(i, j) \in \mathcal{S}'$, then the resulting C_{ij} will be large. In contrast, C_{ij} will become small for any $(i, j) \in \mathcal{S}$. Therefore, we conclude that Condition (A.2) can always hold given a suitable function ψ and enough samples.

It is known that *incoherence* conditions are almost necessary for the ℓ_1 -norm based methods to be support recovery consistent [30, 36, 42, 45, 47]. For example, our previous work [45] with the ℓ_1 -norm regularization requires the *incoherence* condition, also known as the *irrepresentability* condition, on the underlying precision matrix Θ for support recovery consistency, which can be stated as follows,

$$(A.5) \quad \left\| \mathbf{H}_{\mathcal{S}^c\mathcal{S}} (\mathbf{H}_{\mathcal{S}\mathcal{S}})^{-1} \right\|_{\infty} \leq 1 - \eta, \quad \text{for some } \eta \in (0, 1],$$

where \mathbf{H} is the Hessian at Θ , *i.e.*, $\mathbf{H} = \Theta^{-1} \otimes \Theta^{-1}$. We note that the *incoherence* condition (A.5) usually does not hold in practice and is not straightforward to interpret. However, the statements in Theorem A.2 hold without assuming such condition on Θ , while we impose Condition (A.2) on regularization parameters instead, which can always hold as discussed above. Our results are consistent with previous results in linear regression models that the weighted ℓ_1 -regularized methods enjoy the variable selection consistency without requiring *incoherence* condition [48].

Appendix B. Additional experimental results. In this section, we first provide empirical evidence that the minimizer of Problem (2.1) recovers the support of the underlying precision matrix correctly given enough samples and the required sample size has approximate logarithmic dependence on the number of nodes. Then we present the illustration of BA graphs used in numerical experiments of the main article.

B.1. Support recovery consistency. The required sample size in Theorem A.2 is $n \geq cd^2 \log(p)$, where p is the number of nodes and d is the maximum number of nonzero elements in each row or column of Θ . To show that n has approximate logarithmic dependence on p , we conduct experiments on ring and grid graphs, where d is always equal to 3 and 5, respectively, independent of p . To make c approximately constant across a range of different numbers of nodes, we generate constant graph weights and collect them into the weighted adjacency matrix \mathbf{A} . Then we generate the underlying precision matrix Θ by the same procedures as adopted in (5.4) of the main article.

It is observed in Figure 9 that the probability of successful support recovery for each curve transitions from zero to one as the sample size increases, which is consistent with our theoretical results in Theorem A.2 that the minimizer of Problem (2.1) enjoys the support recovery consistency without requiring the *incoherence* condition. We note that all the generated underlying precision matrices Θ do not satisfy the *incoherence* condition in (A.5). We also observe that the curves corresponding to different numbers of nodes all stack up, implying that the ratio $n/\log p$ acts as an effective sample size in controlling the success of support recovery. Therefore, the sample size n required for successful support recovery has approximate logarithmic dependence on p when c remains approximately constant.

B.2. Illustration of BA graphs. In the main article, we use the BA graphs [3] as the model to generate the support of the underlying precision matrix. To help readers to know well the BA graphs, we present two examples in Figure 10, which are the BA graphs with degree one and two, consisting of 500 nodes. Note that a BA

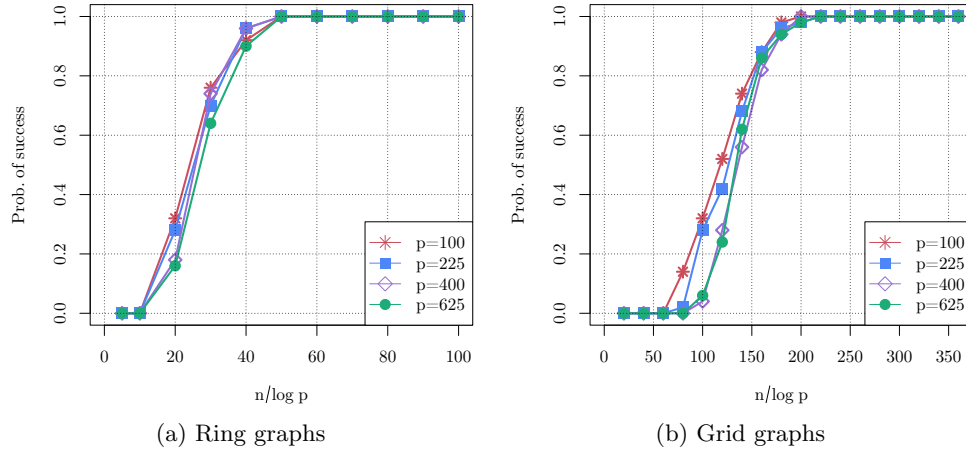


Fig. 9: Probability of successful support recovery as a function of the sample size ratio $n / \log p$ on (a) ring graphs, and (b) grid graphs. All results are averaged over 50 realizations.

graph of degree r indicates that each new node is connected to r existing nodes with a probability that is proportional to the number of edges that the existing nodes already have, which follows the *preferential attachment* mechanism.

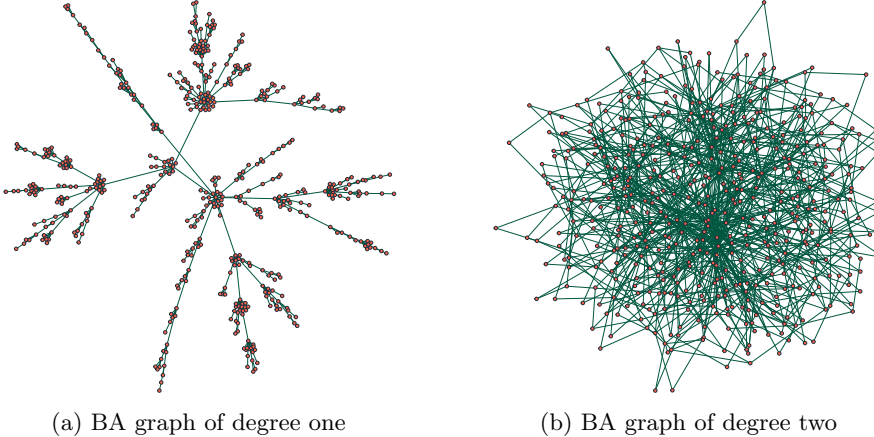


Fig. 10: Illustration of the generated BA graph of degree one in (a), and BA graphs of degree two in (b), both consisting of 500 nodes.

Appendix C. Proof of Theorem A.2.

Proof. Recall that the \mathbf{X}^* is the minimizer of Problem (2.1). We define an oracle estimator $\hat{\mathbf{X}}$ by

$$(C.1) \quad \begin{aligned} \hat{\mathbf{X}} := \arg \min_{\mathbf{X} \in \mathcal{M}^p} \quad & -\log \det(\mathbf{X}) + \text{tr}(\mathbf{X}\mathbf{S}) + \sum_{i \neq j} \lambda_{ij} |X_{ij}|, \\ \text{subject to} \quad & X_{ij} = 0, \quad \forall (i, j) \in \mathcal{S}^c, \end{aligned}$$

where \mathcal{S}^c is the complement of the support set of the underlying precision matrix Θ . Note that the set \mathcal{S}^c only contains the indexes of the off-diagonal elements because of the fact that $\Theta \in \mathcal{M}^p$.

The Lagrangian of the optimization (C.1) is

$$\hat{L}(\mathbf{X}, \mathbf{Y}) = -\log \det(\mathbf{X}) + \text{tr}(\mathbf{X}\mathbf{S}) - \sum_{i \neq j} \lambda_{ij} X_{ij} + \langle \mathbf{Y}, \mathbf{X} \rangle,$$

where \mathbf{Y} is a KKT multiplier with $Y_{ii} = 0$ for $i \in [p]$. With a similar argument for the KKT system in (4.3)-(4.6) for Problem (2.1), the pair $(\hat{\mathbf{X}}, \hat{\mathbf{Y}})$ is primal and dual optimal if and only if it satisfies the KKT system of (C.1) as below

$$(C.2) \quad -\hat{\mathbf{X}}^{-1} + \mathbf{S} - \boldsymbol{\lambda} + \hat{\mathbf{Y}} = \mathbf{0};$$

$$(C.3) \quad \hat{X}_{ij} = 0, \quad \forall (i, j) \in \mathcal{S}^c;$$

$$(C.4) \quad \hat{X}_{ij} \hat{Y}_{ij} = 0, \quad \hat{X}_{ij} \leq 0, \quad \hat{Y}_{ij} \geq 0, \quad \forall (i, j) \in \mathcal{S}_{\text{off}};$$

$$(C.5) \quad \hat{Y}_{ii} = 0, \quad \forall i \in [p];$$

where $\mathcal{S}_{\text{off}} = \{(i, j) \in [p]^2 \mid \Theta_{ij} < 0, i \neq j\}$, i.e., the set of indexes corresponding to the nonzero off-diagonal elements of Θ . Recall that $\mathcal{S}' = \mathcal{S}^c \setminus \mathcal{E}$ and $\mathcal{E} \subseteq \mathcal{S}^c$. Then we can check that, if

$$(C.6) \quad \hat{Y}_{ij} = [\hat{\mathbf{X}}^{-1}]_{ij} - S_{ij} + \lambda_{ij} \geq 0$$

holds for any $(i, j) \in \mathcal{S}'$, then $(\hat{\mathbf{X}}, \hat{\mathbf{Y}})$ also satisfies the KKT system of (2.1) as shown in (4.3)-(4.6), implying that $\mathbf{X}^* = \hat{\mathbf{X}}$.

In what follows, we aim to establish (C.6). Define a function $h : \mathbb{R}^{|\mathcal{S}|} \rightarrow \mathbb{R}^{|\mathcal{S}|}$,

$$h(\boldsymbol{\Delta}_{\mathcal{S}}) = - \left[(\boldsymbol{\Theta} + \widetilde{\boldsymbol{\Delta}}_{\mathcal{S}})^{-1} \right]_{\mathcal{S}} + \mathbf{S}_{\mathcal{S}} - \boldsymbol{\lambda}_{\mathcal{S}},$$

where the notation $\mathbf{X}_{\mathcal{S}} \in \mathbb{R}^{|\mathcal{S}|}$ denotes a vector containing all the elements of \mathbf{X} in the set \mathcal{S} , and $\widetilde{\mathbf{X}}_{\mathcal{S}} \in \mathbb{R}^{p \times p}$ denotes a matrix defined by

$$\left[\widetilde{\mathbf{X}}_{\mathcal{S}} \right]_{ij} = \begin{cases} X_{ij} & \text{if } (i, j) \in \mathcal{S}, \\ 0 & \text{otherwise.} \end{cases}$$

Define a function $g : \mathbb{R}^{|\mathcal{S}|} \rightarrow \mathbb{R}^{|\mathcal{S}|}$

$$(C.7) \quad g(\boldsymbol{\Delta}_{\mathcal{S}}) = -(\mathbf{H}_{\mathcal{S}\mathcal{S}})^{-1} h(\boldsymbol{\Delta}_{\mathcal{S}}) + \boldsymbol{\Delta}_{\mathcal{S}},$$

where \mathbf{H} is the Hessian matrix at $\boldsymbol{\Theta}$. We consider a region

(C.8)

$$\mathcal{B}(r) := \left\{ \boldsymbol{\Delta}_{\mathcal{S}} \in \mathbb{R}^{|\mathcal{S}|} \mid \|\boldsymbol{\Delta}_{\mathcal{S}}\|_{\max} \leq r, \widetilde{\boldsymbol{\Delta}}_{\mathcal{S}} = \widetilde{\boldsymbol{\Delta}}_{\mathcal{S}}^{\top} \right\}, \quad \text{with } r := \frac{4}{3} K_H \|\boldsymbol{\lambda}_{\mathcal{S}}\|_{\max}.$$

Recall that we specify the regularization parameter $\lambda_{ij} = C_{ij} \sqrt{\frac{\log p}{n}}$, where C_{ij} is a positive constant. Let $c_1 = \max_{(i,j) \in \mathcal{S}} |C_{ij}|$. Then we have $\|\boldsymbol{\lambda}_{\mathcal{S}}\|_{\max} = c_1 \sqrt{\frac{\log p}{n}}$. When the sample size is lower bounded by

(C.9)

$$n \geq cd^2 \log p \quad \text{with } c = \left(4c_1 K_H K_{\Sigma} \max \left(4K_H K_{\Sigma}^2 \max \left(\frac{\|\boldsymbol{\lambda}_{\mathcal{S}}\|_{\max}}{\|\boldsymbol{\lambda}_{\mathcal{S}'}\|_{\min}}, 1 \right), 1 \right) \right)^2,$$

we have

$$(C.10) \quad r \leq \min \left(\frac{1}{3dK_\Sigma}, \frac{1}{12dK_H K_\Sigma^3} \min \left(1, \frac{\|C_{S'}\|_{\min}}{\|C_S\|_{\max}} \right) \right).$$

For any $\Delta_S \in \mathcal{B}(r)$, we have

$$(C.11) \quad \left\| \Theta^{-1} \widetilde{\Delta}_S \right\|_\infty \leq \left\| \Theta^{-1} \right\|_\infty \left\| \widetilde{\Delta}_S \right\|_\infty \leq K_\Sigma d \left\| \Delta_S \right\|_{\max} \leq \frac{1}{3},$$

where the second inequality follows from the definition of K_Σ in (A.1) and the fact that Θ has at most d nonzero elements in any row, and the last inequality follows from (C.10). The (C.11) can guarantee that $(\Theta + \widetilde{\Delta}_S)^{-1}$ is invertible. We can further obtain the convergent matrix expansion,

$$(C.12) \quad \begin{aligned} (\Theta + \widetilde{\Delta}_S)^{-1} &= (\mathbf{I} + \Theta^{-1} \widetilde{\Delta}_S)^{-1} \Theta^{-1} \\ &= \sum_{k=0}^{\infty} (-1)^k (\Theta^{-1} \widetilde{\Delta}_S)^k \Theta^{-1} \\ &= \Theta^{-1} - \Theta^{-1} \widetilde{\Delta}_S \Theta^{-1} + \sum_{k=2}^{\infty} (-1)^k (\Theta^{-1} \widetilde{\Delta}_S)^k \Theta^{-1} \\ &= \Theta^{-1} - \Theta^{-1} \widetilde{\Delta}_S \Theta^{-1} + \Theta^{-1} \widetilde{\Delta}_S \Theta^{-1} \widetilde{\Delta}_S N \Theta^{-1}, \end{aligned}$$

where $N = \sum_{k=0}^{\infty} (-1)^k (\Theta^{-1} \widetilde{\Delta}_S)^k$. Define $R(\Delta)$ as

$$(C.13) \quad R(\Delta) = (\Theta + \Delta)^{-1} - \Theta^{-1} + \Theta^{-1} \Delta \Theta^{-1}.$$

Then we have

$$\begin{aligned} R(\widetilde{\Delta}_S) &= (\Theta + \widetilde{\Delta}_S)^{-1} - \Theta^{-1} + \Theta^{-1} \widetilde{\Delta}_S \Theta^{-1} \\ &= \Theta^{-1} \widetilde{\Delta}_S \Theta^{-1} \widetilde{\Delta}_S N \Theta^{-1}, \end{aligned}$$

where the second equality follows from (C.12). We now bound the term $R(\widetilde{\Delta}_S)$ as follows

$$\begin{aligned} \left\| R(\widetilde{\Delta}_S) \right\|_{\max} &= \max_{i,j} \left| e_i^\top \Theta^{-1} \widetilde{\Delta}_S \Theta^{-1} \widetilde{\Delta}_S N \Theta^{-1} e_j \right| \\ &\leq \max_i \left\| e_i^\top \Theta^{-1} \widetilde{\Delta}_S \right\|_{\max} \max_j \left\| \Theta^{-1} \widetilde{\Delta}_S N \Theta^{-1} e_j \right\|_1 \\ &\leq \max_i \left\| e_i^\top \Theta^{-1} \right\|_1 \left\| \widetilde{\Delta}_S \right\|_{\max} \max_j \left\| \Theta^{-1} \widetilde{\Delta}_S N \Theta^{-1} e_j \right\|_1 \\ &= \left\| \Theta^{-1} \right\|_\infty \left\| \widetilde{\Delta}_S \right\|_{\max} \left\| \Theta^{-1} \widetilde{\Delta}_S N \Theta^{-1} \right\|_1 \\ &\leq \left\| \widetilde{\Delta}_S \right\|_{\max} \left\| \widetilde{\Delta}_S \right\|_\infty \left\| N^\top \right\|_\infty \left\| \Theta^{-1} \right\|_\infty^3 \\ &\leq \frac{3}{2} d K_\Sigma^3 \left\| \Delta_S \right\|_{\max}^2, \end{aligned}$$

where the first inequality follows from the fact that $|a^\top b| \leq \|a\|_{\max} \|b\|_1$ holds for any $a, b \in \mathbb{R}^p$; the second inequality is established by the inequality that $\|a^\top B\|_{\max} \leq$

$\|\mathbf{a}\|_1 \|\mathbf{B}\|_{\max}$ for any $\mathbf{a} \in \mathbb{R}^p$ and $\mathbf{B} \in \mathbb{R}^{p \times q}$; the third inequality follows from $\|\mathbf{A}\|_1 = \|\mathbf{A}^\top\|_\infty$ and the sub-multiplicativity of $\|\cdot\|_\infty$; the last inequality follows from $\|\widetilde{\Delta}_S\|_\infty \leq d \|\widetilde{\Delta}_S\|_{\max}$ since there are at most d nonzero elements in each row and column of $\widetilde{\Delta}_S$, and the bound of the term $\|\mathbf{N}^\top\|_\infty$ in the following

$$\|\mathbf{N}^\top\|_\infty \leq \sum_{k=0}^{\infty} \|\widetilde{\Delta}_S \Theta^{-1}\|_\infty^k \leq \frac{1}{1 - \|\widetilde{\Delta}_S\|_\infty \|\Theta^{-1}\|_\infty} \leq \frac{3}{2},$$

where the last inequality follows from (C.11).

For any $\Delta_S \in \mathbb{B}(r)$ with $r \leq \min\left(\frac{1}{3dK_\Sigma}, \frac{1}{12dK_HK_\Sigma^3} \min\left(1, \frac{\|C_{S'}\|_{\min}}{\|C_S\|_{\max}}\right)\right)$, we have

$$(C.14) \quad \|\mathbf{R}(\widetilde{\Delta}_S)\|_{\max} \leq \frac{r}{8K_H} \min\left(1, \frac{\|C_{S'}\|_{\min}}{\|C_S\|_{\max}}\right) = \frac{1}{6} \min(\|\lambda_S\|_{\max}, \|\lambda_{S'}\|_{\min}),$$

where the equality follows from the definition of r in (C.8).

We can rewrite the function g in (C.7) as

$$\begin{aligned} g(\Delta_S) &= -(\mathbf{H}_{SS})^{-1} \left(-\left[(\Theta + \widetilde{\Delta}_S)^{-1} \right]_S + \mathbf{S}_S - \lambda_S \right) + \Delta_S \\ &= -(\mathbf{H}_{SS})^{-1} \left(-[\Theta^{-1}]_S + \left[\Theta^{-1} \widetilde{\Delta}_S \Theta^{-1} \right]_S \right. \\ &\quad \left. - \left[\Theta^{-1} \widetilde{\Delta}_S \Theta^{-1} \widetilde{\Delta}_S \mathbf{N} \Theta^{-1} \right]_S + \mathbf{S}_S - \lambda_S \right) + \Delta_S. \end{aligned}$$

Following from the fact that

$$\text{vec}(\Theta^{-1} \Delta \Theta^{-1}) = (\Theta^{-1} \otimes \Theta^{-1}) \text{vec}(\Delta) = \mathbf{H} \text{vec}(\Delta),$$

we can obtain

$$(C.15) \quad \left[\Theta^{-1} \widetilde{\Delta}_S \Theta^{-1} \right]_S = \mathbf{H}_{SS} \Delta_S.$$

Let $\mathbf{G} = \mathbf{S} - \Theta^{-1}$. Following from (C.15), we obtain

$$g(\Delta_S) = (\mathbf{H}_{SS})^{-1} \left(\left[\mathbf{R}(\widetilde{\Delta}_S) \right]_S - \mathbf{G}_S + \lambda_S \right).$$

For any $\Delta_S \in \mathcal{B}(r)$, we bound $g(\Delta_S)$ as follows,

$$\begin{aligned} \|g(\Delta_S)\|_{\max} &\leq \left\| (\mathbf{H}_{SS})^{-1} \right\|_\infty \left(\left\| \left[\mathbf{R}(\widetilde{\Delta}_S) \right]_S \right\|_{\max} + \|\mathbf{G}_S\|_{\max} + \|\lambda_S\|_{\max} \right) \\ (C.16) \quad &\leq K_H \left(\frac{1}{3} \min(\|\lambda_S\|_{\max}, \|\lambda_{S'}\|_{\min}) + \|\lambda_S\|_{\max} \right) \\ &\leq r, \end{aligned}$$

where the second inequality follows from the condition in (A.3) that

$$(C.17) \quad \|\mathbf{G}\|_{\max} \leq \frac{1}{6} \min(\|\lambda_S\|_{\max}, \|\lambda_{S'}\|_{\min}),$$

and (C.14), and the last inequality in (C.16) follows from the definition of r in (C.8). We also have

$$\left[\mathbf{R}(\widetilde{\Delta}_S) \right]_S - \mathbf{G}_S + \boldsymbol{\lambda}_S = \left[\Theta^{-1} \widetilde{g(\Delta_S)} \Theta^{-1} \right]_S = \left[\Theta^{-1} \widetilde{g(\Delta_S)}^\top \Theta^{-1} \right]_S,$$

where the last equality follows from the fact that $\mathbf{R}(\widetilde{\Delta}_S)$, \mathbf{G} and $\boldsymbol{\lambda}$ are all symmetric. Since $g(\Delta_S)$ is injective, we can obtain

$$\widetilde{g(\Delta_S)} = \widetilde{g(\Delta_S)}^\top.$$

Together with (C.16), we conclude that $g(\Delta_S) \in \mathcal{B}(r)$ for any $\Delta_S \in \mathcal{B}(r)$. Therefore, $g(\Delta_S)$ is a continuous self mapping in the convex compact set $\mathcal{B}(r)$. Following from the Brouwer fixed-point theorem, we obtain that there exists a fixed point $\bar{\Delta}_S$ such that $g(\bar{\Delta}_S) = \bar{\Delta}_S$, i.e., $h(\bar{\Delta}_S) = \mathbf{0}$. Then we have

$$(C.18) \quad - \left[\left(\Theta + \widetilde{\bar{\Delta}_S} \right)^{-1} \right]_S + \mathbf{S}_S - \boldsymbol{\lambda}_S = \mathbf{0}.$$

We construct $\hat{\mathbf{X}}$ by

$$\hat{\mathbf{X}} = \Theta + \widetilde{\bar{\Delta}_S},$$

and $\hat{\mathbf{Y}}$ by

$$\hat{Y}_{ij} = \begin{cases} \left[\hat{\mathbf{X}}^{-1} - \mathbf{S} + \boldsymbol{\lambda} \right]_{ij} & \text{if } (i, j) \in \mathcal{S}^c, \\ 0 & \text{otherwise.} \end{cases}$$

We can check that this pair $(\hat{\mathbf{X}}, \hat{\mathbf{Y}})$ satisfies the KKT system of Problem (C.1) as shown in (C.2)-(C.5). Note that we have

$$(C.19) \quad \hat{X}_{ij} < 0, \quad \forall (i, j) \in \mathcal{S}_{\text{off}},$$

which follows from Assumption A.1 that $\min_{(i,j) \in \mathcal{S}_{\text{off}}} |\Theta_{ij}| > \frac{4}{3} K_H \|\boldsymbol{\lambda}_S\|_{\max}$.

According to (C.13), one obtains

$$\mathbf{R}(\widetilde{\bar{\Delta}_S}) = \hat{\mathbf{X}}^{-1} - \Theta^{-1} + \Theta^{-1} \widetilde{\bar{\Delta}_S} \Theta^{-1}.$$

Let $\boldsymbol{\Xi} = \hat{\mathbf{X}}^{-1} - \mathbf{S}$. Then we obtain

$$(C.20) \quad \Theta^{-1} \widetilde{\bar{\Delta}_S} \Theta^{-1} - \mathbf{R}(\widetilde{\bar{\Delta}_S}) + \mathbf{G} + \boldsymbol{\Xi} = \mathbf{0}.$$

We can rewrite (C.20) by *vectorizing* the matrices, and get

$$\mathbf{H} \text{vec}(\widetilde{\bar{\Delta}_S}) - \text{vec}(\mathbf{R}(\widetilde{\bar{\Delta}_S})) + \text{vec}(\mathbf{G}) + \text{vec}(\boldsymbol{\Xi}) = \mathbf{0}.$$

We decompose the equality into two blocks with respect to \mathcal{S} and \mathcal{S}' and obtain

$$\mathbf{H}_{\mathcal{S}\mathcal{S}} \bar{\Delta}_S - \left[\mathbf{R}(\widetilde{\bar{\Delta}_S}) \right]_S + \mathbf{G}_S + \boldsymbol{\Xi}_S = \mathbf{0},$$

and

$$\mathbf{H}_{\mathcal{S}'\mathcal{S}}\bar{\boldsymbol{\Delta}}_{\mathcal{S}} - \left[\mathbf{R}\left(\widetilde{\boldsymbol{\Delta}}_{\mathcal{S}}\right)\right]_{\mathcal{S}'} + \mathbf{G}_{\mathcal{S}'} + \boldsymbol{\Xi}_{\mathcal{S}'} = \mathbf{0}.$$

By eliminating $\bar{\boldsymbol{\Delta}}_{\mathcal{S}}$, we can get

$$\begin{aligned} (C.21) \quad \|\boldsymbol{\Xi}_{\mathcal{S}'}\|_{\max} &\leq \left\| \mathbf{H}_{\mathcal{S}'\mathcal{S}}(\mathbf{H}_{\mathcal{S}\mathcal{S}})^{-1} \right\|_{\infty} \left(\|\mathbf{G}_{\mathcal{S}}\|_{\max} + \left\| \left[\mathbf{R}\left(\widetilde{\boldsymbol{\Delta}}_{\mathcal{S}}\right)\right]_{\mathcal{S}} \right\|_{\max} \right) \\ &\quad + \left\| \mathbf{H}_{\mathcal{S}'\mathcal{S}}(\mathbf{H}_{\mathcal{S}\mathcal{S}})^{-1}\boldsymbol{\Xi}_{\mathcal{S}} \right\|_{\max} + \left(\|\mathbf{G}_{\mathcal{S}'}\|_{\max} + \left\| \left[\mathbf{R}\left(\widetilde{\boldsymbol{\Delta}}_{\mathcal{S}}\right)\right]_{\mathcal{S}'} \right\|_{\max} \right). \end{aligned}$$

According to (C.18), we have

$$\|\boldsymbol{\Xi}_{\mathcal{S}}\|_{\max} = \|\boldsymbol{\lambda}_{\mathcal{S}}\|_{\max}.$$

Combining (C.14), (C.17) and (C.21) yields

$$(C.22) \quad \|\boldsymbol{\Xi}_{\mathcal{S}'}\|_{\max} \leq \frac{4}{3} \left\| \mathbf{H}_{\mathcal{S}'\mathcal{S}}(\mathbf{H}_{\mathcal{S}\mathcal{S}})^{-1} \right\|_{\infty} \|\boldsymbol{\lambda}_{\mathcal{S}}\|_{\max} + \frac{1}{3} \|\boldsymbol{\lambda}_{\mathcal{S}'}\|_{\min} \leq \|\boldsymbol{\lambda}_{\mathcal{S}'}\|_{\min},$$

where the last inequality follows from the condition that

$$\frac{\|\boldsymbol{\lambda}_{\mathcal{S}'}\|_{\min}}{\|\boldsymbol{\lambda}_{\mathcal{S}}\|_{\max}} = \frac{\|C_{\mathcal{S}'}\|_{\min}}{\|C_{\mathcal{S}}\|_{\max}} \geq 2 \left\| \mathbf{H}_{\mathcal{S}'\mathcal{S}}(\mathbf{H}_{\mathcal{S}\mathcal{S}})^{-1} \right\|_{\infty}.$$

By establishing (C.22), we obtain

$$\max_{(i,j) \in \mathcal{S}'} \left| [\hat{\mathbf{X}}^{-1}]_{ij} - S_{ij} \right| \leq \min_{(i,j) \in \mathcal{S}'} \lambda_{ij}.$$

Therefore, we can conclude that (C.6) holds. As a result, we obtain that $\mathbf{X}^* = \hat{\mathbf{X}}$.

According to the definition of $\hat{\mathbf{X}}$ in (C.1), we get that for any $(i,j) \in \mathcal{S}^c$, where $\mathcal{S}^c = \{(i,j) \mid \Theta_{ij} = 0\}$, we have $[\hat{\mathbf{X}}]_{ij} = 0$. Meanwhile, following from (C.19) and the fact that $[\hat{\mathbf{X}}]_{ii} \neq 0$ for any $i \in [p]$, we have $[\hat{\mathbf{X}}]_{ij} \neq 0$ for any $(i,j) \in \mathcal{S}$. Therefore, we can establish that $\text{supp}(\hat{\mathbf{X}}) = \text{supp}(\boldsymbol{\Theta})$, and thus $\text{supp}(\mathbf{X}^*) = \text{supp}(\boldsymbol{\Theta})$. \square

Acknowledgments. We would like to thank Eduardo Pavez for providing the optGL code, and thank Brenden M. Lake for providing the concepts data set.

REFERENCES

- [1] R. AGRAWAL, U. ROY, AND C. UHLER, *Covariance Matrix Estimation under Total Positivity for Portfolio Selection*, Journal of Financial Econometrics, 20 (2020), pp. 367–389.
- [2] O. BANERJEE, L. E. GHAOUI, AND A. D’ASPREMONT, *Model selection through sparse maximum likelihood estimation for multivariate Gaussian or binary data*, Journal of Machine Learning Research, 9 (2008), pp. 485–516.
- [3] A.-L. BARABÁSI AND R. ALBERT, *Emergence of scaling in random networks*, Science, 286 (1999), pp. 509–512.
- [4] J. M. BARDSLEY AND C. R. VOGEL, *A nonnegatively constrained convex programming method for image reconstruction*, SIAM Journal on Scientific Computing, 25 (2004), pp. 1326–1343.
- [5] D. P. BERTSEKAS, *On the Goldstein-Levitin-Polyak gradient projection method*, IEEE Transactions on Automatic Control, 21 (1976), pp. 174–184.

- [6] D. P. BERTSEKAS, *Projected Newton methods for optimization problems with simple constraints*, SIAM Journal on Control and Optimization, 20 (1982), pp. 221–246.
- [7] D. P. BERTSEKAS, *Nonlinear programming*, Athena Scientific, Belmont, MA, third ed., 2016.
- [8] E. J. CANDES, M. B. WAKIN, AND S. P. BOYD, *Enhancing sparsity by reweighted ℓ_1 minimization*, Journal of Fourier analysis and applications, 14 (2008), pp. 877–905.
- [9] A. D'ASPREMONT, O. BANERJEE, AND L. EL GHAOUI, *First-order methods for sparse covariance selection*, SIAM Journal on Matrix Analysis and Applications, 30 (2008), pp. 56–66.
- [10] Q. T. DINH, A. KYRILLIDIS, AND V. CEVHER, *A proximal Newton framework for composite minimization: Graph learning without Cholesky decompositions and matrix inversions*, in International Conference on Machine Learning, vol. 28, 2013, pp. 271–279.
- [11] P. DRÁBEK AND J. MILOTA, *Methods of nonlinear analysis: applications to differential equations*, Springer Science & Business Media, 2007.
- [12] J. DUCHI, S. GOULD, AND D. KOLLER, *Projected subgradient methods for learning sparse Gaussians*, in Conference on Uncertainty in Artificial Intelligence, 2008, p. 153–160.
- [13] H. E. EGILMEZ, E. PAVEZ, AND A. ORTEGA, *Graph learning from data under Laplacian and structural constraints*, IEEE Journal of Selected Topics in Signal Processing, 11 (2017), pp. 825–841.
- [14] S. FALLAT, S. LAURITZEN, K. SADEGH, C. UHLER, N. WERMUTH, AND P. ZWIERNIK, *Total positivity in Markov structures*, The Annals of Statistics, 45 (2017), pp. 1152–1184.
- [15] J. FRIEDMAN, T. HASTIE, AND R. TIBSHIRANI, *Sparse inverse covariance estimation with the graphical lasso*, Biostatistics, 9 (2008), pp. 432–441.
- [16] E. M. GAFNI AND D. P. BERTSEKAS, *Two-metric projection methods for constrained optimization*, SIAM Journal on Control and Optimization, 22 (1984), pp. 936–964.
- [17] J. L. HERRING, J. NAGY, AND L. RUTHOTTO, *Gauss–Newton optimization for phase recovery from the bispectrum*, IEEE Transactions on Computational Imaging, 6 (2019), pp. 235–247.
- [18] C.-J. HSIEH, M. A. SUSTIK, I. S. DHILLON, AND P. RAVIKUMAR, *QUIC: quadratic approximation for sparse inverse covariance estimation*, The Journal of Machine Learning Research, 15 (2014), pp. 2911–2947.
- [19] Á. B. JIMÉNEZ AND S. SRA, *Fast Newton-type methods for total variation regularization*, in International Conference on Machine Learning, 2011, pp. 313–320.
- [20] J. KELNER, F. KOEHLER, R. MEKA, AND A. MOITRA, *Learning some popular Gaussian graphical models without condition number bounds*, in Advances in Neural Information Processing Systems, vol. 33, 2020, pp. 10986–10998.
- [21] D. KIM, S. SRA, AND I. S. DHILLON, *Fast Newton-type methods for the least squares nonnegative matrix approximation problem*, in SIAM International Conference on Data Mining, 2007, pp. 343–354.
- [22] D. KIM, S. SRA, AND I. S. DHILLON, *Tackling box-constrained optimization via a new projected Quasi-Newton approach*, SIAM Journal on Scientific Computing, 32 (2010), pp. 3548–3563.
- [23] S. KUMAR, J. YING, J. V. D. M. CARDOSO, AND D. P. PALOMAR, *A unified framework for structured graph learning via spectral constraints*, Journal of Machine Learning Research, 21 (2020), pp. 1–60.
- [24] B. LAKE AND J. TENENBAUM, *Discovering structure by learning sparse graphs*, in Proceedings of the 33rd Annual Cognitive Science Conference, 2010, pp. 778–783.
- [25] G. LANDI AND E. L. PICCOLOMINI, *An improved Newton projection method for nonnegative deblurring of Poisson-corrupted images with Tikhonov regularization*, Numerical Algorithms, 60 (2012), pp. 169–188.
- [26] S. LAURITZEN, C. UHLER, AND P. ZWIERNIK, *Maximum likelihood estimation in Gaussian models under total positivity*, The Annals of Statistics, 47 (2019), pp. 1835–1863.
- [27] S. LAURITZEN, C. UHLER, AND P. ZWIERNIK, *Total positivity in exponential families with application to binary variables*, The Annals of Statistics, 49 (2021), pp. 1436–1459.
- [28] L. LI AND K.-C. TOH, *An inexact interior point method for L_1 -regularized sparse covariance selection*, Mathematical Programming Computation, 2 (2010), pp. 291–315.
- [29] Z. LU, *Smooth optimization approach for sparse covariance selection*, SIAM Journal on Optimization, 19 (2009), pp. 1807–1827.
- [30] N. MEINSHAUSEN AND P. BÜHLMANN, *High-dimensional graphs and variable selection with the lasso*, The Annals of Statistics, 34 (2006), pp. 1436–1462.
- [31] Y. NESTEROV, *Introductory lectures on convex optimization: A basic course*, vol. 87, Springer Science & Business Media, 2003.
- [32] M. E. NEWMAN, *Modularity and community structure in networks*, Proceedings of the National Academy of Sciences, 103 (2006), pp. 8577–8582.
- [33] E. PAVEZ, H. E. EGILMEZ, AND A. ORTEGA, *Learning graphs with monotone topology properties and multiple connected components*, IEEE Transactions on Signal Processing, 66 (2018),

- pp. 2399–2413.
- [34] E. PAVEZ AND A. ORTEGA, *Generalized Laplacian precision matrix estimation for graph signal processing*, in 2016 IEEE International Conference on Acoustics, Speech and Signal Processing, 2016, pp. 6350–6354.
- [35] R. J. PLEMMONS, *M-matrix characterizations. i—nonsingular m-matrices*, Linear Algebra and its applications, 18 (1977), pp. 175–188.
- [36] P. RAVIKUMAR, M. J. WAINWRIGHT, G. RASKUTTI, AND B. YU, *High-dimensional covariance estimation by minimizing ℓ_1 -penalized log-determinant divergence*, Electronic Journal of Statistics, 5 (2011), pp. 935–980.
- [37] D. ROTHERMEL AND T. SCHUSTER, *Solving an inverse heat convection problem with an implicit forward operator by using a projected quasi-Newton method*, Inverse Problems, 37 (2021), p. 045014.
- [38] K. SCHEINBERG, S. MA, AND D. GOLDFARB, *Sparse inverse covariance selection via alternating linearization methods*, in Advances in Neural Information Processing Systems, vol. 23, 2010, pp. 2101–2109.
- [39] G. SCUTARI, F. FACCHINEI, P. SONG, D. P. PALOMAR, AND J.-S. PANG, *Decomposition by partial linearization: Parallel optimization of multi-agent systems*, IEEE Transactions on Signal Processing, 62 (2014), pp. 641–656.
- [40] D. I. SHUMAN, S. K. NARANG, P. FROSSARD, A. ORTEGA, AND P. VANDERGHEYNST, *The emerging field of signal processing on graphs: Extending high-dimensional data analysis to networks and other irregular domains*, IEEE Signal Processing Magazine, 30 (2013), pp. 83–98.
- [41] M. SLAWSKI AND M. HEIN, *Estimation of positive definite M-matrices and structure learning for attractive Gaussian Markov random fields*, Linear Algebra and its Applications, 473 (2015), pp. 145–179.
- [42] J. A. TROPP, *Just relax: Convex programming methods for identifying sparse signals in noise*, IEEE Transactions on Information Theory, 52 (2006), pp. 1030–1051.
- [43] C. WANG, D. SUN, AND K.-C. TOH, *Solving log-determinant optimization problems by a Newton-CG primal proximal point algorithm*, SIAM Journal on Optimization, 20 (2010), pp. 2994–3013.
- [44] Y. WANG, U. ROY, AND C. UHLER, *Learning high-dimensional Gaussian graphical models under total positivity without adjustment of tuning parameters*, in International Conference on Artificial Intelligence and Statistics, vol. 108, 2020, pp. 2698–2708.
- [45] J. YING, J. V. D. M. CARDOSO, AND D. P. PALOMAR, *A fast algorithm for graph learning under attractive Gaussian Markov random fields*, in 2021 55th Asilomar Conference on Signals, Systems, and Computers, 2021.
- [46] M. YUAN AND Y. LIN, *Model selection and estimation in the Gaussian graphical model*, Biometrika, 94 (2007), pp. 19–35.
- [47] P. ZHAO AND B. YU, *On model selection consistency of Lasso*, The Journal of Machine Learning Research, 7 (2006), pp. 2541–2563.
- [48] H. ZOU, *The adaptive lasso and its oracle properties*, Journal of the American Statistical Association, 101 (2006), pp. 1418–1429.